

Revisiting the Hydrological Basis of the Budyko Framework With the Hydrologically Similar Groups Principle

Yuchan Chen¹, Xiuzhi Chen¹, Meimei Xue¹, Chuanxun Yang^{2,3}, Wei Zheng¹, Jun Cao⁴, Wenting Yan¹,
[Wenping Yuan¹](#)

¹Guangdong Province Key Laboratory for Climate Change and Natural Disaster Studies, School of Atmospheric Sciences, Sun Yat-sen University, Zhuhai, 519082, China;

²Guangzhou Institute of Geochemistry, Chinese Academy of Sciences, Guangzhou, 510640, China;

³University of Chinese Academy of Sciences, Beijing, 100049, China;

⁴Guangdong provincial Academy of Environmental Science, Guangzhou, 510635, China;

Correspondence to: Xiuzhi Chen (chenxzh73@mail.sysu.edu.cn)

Abstract. The Budyko framework is a simple ~~but~~ and effective tool for ~~estimating the watershed water balance estimation.~~ ~~Accurate estimation.~~ Quantification of the watershed characteristic-related parameter (Pw) is critical to accurate water balance simulations by using the Budyko framework. However, there is no universal ~~quantification criterion method~~ for calculating the Pw ~~because of~~ as the ~~complex~~ interactions between hydrologic, climatic, and watershed characteristic factors ~~at global scales~~ differ greatly between watersheds globally. ~~Therefore, To fill this research gap, this research this study~~ introduced the hydrologically similar groups principle into the Budyko framework and ~~defined the criteria provided a framework~~ for quantifying the Pw of watersheds in similar environments. We firstly classified ~~global~~ the selected 366 watersheds worldwide into six hydrologically similar groups based on watershed attributes, including climate, soil moisture, and vegetation, ~~and identified the~~. Results show that soil moisture (SM) and fractional vegetation cover (FVC) are two controlling factors of the Pw in each group hydrologically similar group. Our results show that the Pw is closely related to soil moisture (SM) and the power function gradually changes from positive to negative as soil moisture increases. The Pw values in dry watersheds (SM<20mm) monotonically increase with SM but in humid watersheds (SM>20mm) convert to monotonically decrease with SM. in power functions. ~~The relationship between the Pw and fractional vegetation cover (FVC) can be described with different linear equations in different hydrologic similarity groups~~ And the FVC shows linearly correlated with the Pw values of watersheds in most hydrologically similar groups, except in ~~the group those~~ with no strong seasonality and moist soils. ~~Based on these relationships, a model for estimating the Pw (PwM) was established with~~ Then, multiple non-linear regression ~~methods~~ models between ~~the~~ Pw and ~~its~~ the controlling factors (SM and FVC) were developed to estimate the Pw for the six hydrologically similar groups individually. ~~Then, we used bootstrapping and reconstruction methods to verify the usability of PwM. The validation results illustrate that PwM overall presents a~~

30 ~~satisfactory performance through bootstrapping ($R^2 = 0.63$) and runoff reconstruction ($R^2 = 0.89$).~~ Cross-validations using
31 the bootstrap sampling method ($R^2 = 0.63$) and validations of time-series GRDC runoff data ($R^2 = 0.89$) both indicate that
32 the proposed models overall present a satisfactory performance of the Pw parameter in the Budyko framework. Results
33 show that the hydrologically similar groups method can quantify the Pw and the improved Budyko framework can aptly
34 simulate global runoff, especially in humid watersheds. Overall, this study is a new attempt to quantify the unknown
35 watershed characteristic-related parameter in the Budyko framework using the hydrologically similar groups method. This
36 study lays the basis for explaining the Pw in the Budyko framework and improves Results will be helpful for improving
37 the applicability of the Budyko framework ~~for in estimating global runoff~~ annual runoff of watersheds in diverse climates
38 and with different characteristics.

39 1 Introduction

40 There has been an increasing interest in estimating the water balance ~~with the Budyko framework (Budyko, 1974)~~
41 ~~because it is of watersheds with~~ a simple and effective tool ~~— the Budyko framework,~~ unlike ~~Unlike the~~ process-based
42 models, ~~which that~~ typically require a large number of parameters as inputs for accurate simulations (Caracciolo et al.,
43 2018; Lei et al., 2014), ~~the Budyko framework is a top-down approach relating a catchment's long-term evaporative ratio~~
44 (ratio between actual evapotranspiration and precipitation) to its aridity index (ratio between potential evapotranspiration
45 and precipitation) and is rooted on a firm physical basis (Vora and Singh, 2021; Sivapalan, 2003; Wang and Tang, 2014).
46 ~~Currently,~~ The the Budyko framework has been widely used for assessing linkages and feedbacks between climate forcing
47 and land surface characteristics on water and energy cycles (Zhang et al., 2001; Milly and Shmakin, 2002; Li et al., 2013;
48 Xu et al., 2013), prompting a great deal of empirical, theoretical, and process-based studies (Chen and Sivapalan, 2020;
49 Roderick and Farquhar, 2011; Rau et al., 2018; Goswami and Goyal, 2022). ~~The Budyko framework is a top-down approach~~
50 ~~relating a catchment's long-term evaporative ratio (ratio between actual evapotranspiration and precipitation) to its aridity~~
51 ~~index (ratio between potential evapotranspiration and precipitation) and is rooted on a firm physical basis (Vora and Singh,~~
52 ~~2021; Sivapalan, 2003; Wang and Tang, 2014).~~

53 The original Budyko equation assumes that evapotranspiration is mainly controlled by precipitation (representing the
54 availability of water) and potential evapotranspiration (representing the availability of energy) (Budyko, 1974; Wang et al.,
55 2022). Despite its solid performance, the original Budyko equation still produces a bias between modeled and measured
56 evapotranspiration or runoff because it does not consider the effects of watershed characteristics other than mean annual

57 climatic conditions on water balance (Kim and Chun, 2021; Zhang et al., 2001). As a result, hydrologists have invested
 58 considerable efforts to improve model performance by introducing parameters related to watershed characteristics
 59 ([watershed characteristic parameter, Pw](#)) into the original Budyko equation. ~~Some of the introduced parametric equations~~
 60 ~~include the Fu (Fu, 1981), Zhang (Zhang et al., 2001), Choudhury Yang (Yang et al., 2008), and Wang Tang equations~~
 61 ~~(Wang and Tang, 2014). The popular parametric equations of the Budyko framework are presented in Table 1.~~

62 **Table 1.** ~~Parametric Budyko type formulations~~ Parametric formulations of the Budyko framework (Pw : watershed characteristic
 63 parameter; ET : actual evaporation, R : runoff, P : precipitation, PET : potential evapotranspiration, all in mm yr⁻¹).

Reference	Formulation	Pw (Theoretical range)	Reference values of Pw
Budyko (1974)	$\frac{ET}{P} = \left[\frac{PET}{P} \tanh \left(\frac{PET}{P} \right)^{-1} (1 - \exp(-\frac{PET}{P})) \right]^{0.5}$	0.5	0.5
Zhang et al. (2001)	$\frac{ET}{P} = \frac{1 + w \frac{PET}{P}}{1 + w \frac{PET}{P} + (\frac{PET}{P})^{-1}}$	w (0, ∞)	Trees – 2.0, Plants – 0.5
Turc (1954), Mezentsev (1955), Choudhury (1999), Yang et al. (2008)	$\frac{ET}{P} = \frac{1}{\left[1 + (\frac{P}{PET})^n \right]^{\frac{1}{n}}}$	n (0, ∞)	Field – 2.6, River basins – 1.8
Wang and Tang (2014)	$\frac{ET}{P} = \frac{1 + \frac{PET}{P} - \sqrt{(1 + \frac{PET}{P})^2 - 4\varepsilon(2 - \varepsilon)\frac{PET}{P}}}{2\varepsilon(2 - \varepsilon)}$	ε (0,1)	0.55 - 0.58
Tixeront (1964), Fu (1981), Zhou et al. (2015a)	$\frac{R}{P} = \left[1 + \left(\frac{P}{PET} \right)^{-m} \right]^{\frac{1}{m}} - \left(\frac{P}{PET} \right)^{-1}$	m (1, ∞)	Forest – 2.83, Shrub – 2.33, Grassland or cropland – 2.28, Mixed land – 2.12

64
 65 ~~These parametric equations have somewhat improved the estimation performance by taking into account the influence~~
 66 ~~of watershed characteristics and thus have better estimation performance (Fu, 1981; Liu and Liang, 2015; Guan et al., 2022;~~
 67 ~~Yang et al., 2008). Along with the widely used parametric equations, there has been a growing importance placed on~~
 68 ~~research on the watershed characteristic parameter (Pw) as its accurate estimation is a prerequisite for the accurate~~
 69 ~~simulation of evapotranspiration or runoff using the Budyko framework (Wang et al., 2022; Yao et al., 2017; Guo et al.,~~
 70 ~~2019; Yu et al., 2021). Although introducing Pw improved the Budyko type model performance, most studies failed to~~
 71 ~~give a specific criterion for quantifying its value. While there is agreement that the Pw represents the integrated effects of~~

72 various environmental factors (Wang et al., 2022; Liu et al., 2022; Yu et al., 2021; Gan et al., 2021), opinions differ as to
73 what factors and effects should relate to the Pw. For instance, whether the Pw within the Budyko framework is controlled
74 by watershed vegetation has been much debated. Some researchers advocated that vegetation plays a crucial role in the Pw,
75 holding that there is a positive linear relationship between vegetation and the Pw (Ning et al., 2017; Zhang et al., 2018;
76 Zhang et al., 2001). Other scholars have argued against vegetation having a strong correlation with the Pw, suggesting that
77 most regions or some special watersheds show no significant correlation between vegetation indices and Pw (Liu et al.,
78 2021; Li et al., 2013). Although many studies have researched the relationship between the Pw and various watershed
79 characteristics factors, they have shown contradictory results.

80 From the hydrological point of view, the Pw controls the fraction of precipitation diverted into the runoff for a given
81 aridity index (Caracciolo et al., 2018). Watersheds with larger Pw values convert larger parts of precipitation to
82 evapotranspiration and consequently less part to runoff than those with smaller Pw values; and some studies defined the
83 Pw as the water retention capacities of watersheds (Fu, 1981; Zhou et al., 2015a). Overall, the Pw denotes the adjustment
84 of water-energy partitioning by watershed characteristics (Yao et al., 2017; Li et al., 2013).

85 During the past decades, researchers have done lots of work to quantify the Pw for the accurate simulation of
86 evapotranspiration or runoff using the Budyko framework (Wang et al., 2022; Yao et al., 2017; Guo et al., 2019; Yu et al.,
87 2021) and made considerable contributions for improving the estimation of Pw by taking into account the influences from
88 watershed characteristics (Fu, 1981; Liu and Liang, 2015; Guan et al., 2022; Yang et al., 2008). Although there is agreement
89 that the Pw represents the integrated effects of various environmental factors (Wang et al., 2022; Liu et al., 2022b; Yu et
90 al., 2021; Gan et al., 2021), studies still differed greatly as to what factors and effects should relate to the Pw and failed to
91 give a general framework for quantifying the Pw. For instance, whether the Pw in the Budyko framework is controlled by
92 vegetation or not has been much debated. Ning et al. (2017) found that the Pw generally had a positive correlation with
93 vegetation coverage. Zhang et al. (2018) obtained the sensitivity of the Pw to changes in LAI by taking a derivative of the
94 Pw function with respect to LAI, implying a crucial role of vegetation cover in impacting the Pw. However, some other
95 studies indicated that most regions or watersheds show no significant influences of vegetation indices or coverage on Pw
96 (Li et al., 2013; Liu et al., 2021). For example, Li et al. (2013) pointed out the variations in the Pw values are not entirely
97 controlled by vegetation coverage in the small catchments. Another study from Liu et al. (2021) also found a weak
98 correlation between the vegetation leaf area index and the Pw. Therefore, more in-depth studies are in need for revisiting
99 the hydrological Basis of Pw in the Budyko Framework.

100 ~~In fact, the relationships and interactions among hydrologic, climatic, and watershed characteristic factors are~~
101 ~~complicated by the great heterogeneity across space (Gao et al., 2018; Gan et al., 2021). Numerous studies have shown~~
102 ~~that the roles of climate and watershed characteristic factors on hydrological characteristics vary in different climatic~~
103 ~~regions (Li and Sivapalan, 2014; Trancoso et al., 2017; Singh et al., 2014). Therefore, classifying watersheds into~~
104 ~~hydrologically similar groups is essential for exploring the effect of watershed characteristics on hydrology and interpreting~~
105 ~~the physical meaning of the Pw within the Budyko framework.~~Here, we hypothesize that watersheds with similar climatic,
106 hydrologic, and watershed-related characteristics have consistent controlling factors of Pw in the Budyko Framework.
107 ~~However, But,~~ to date, ~~relatively little research has~~ very few researches have been conducted on classifying watersheds
108 based on the highly variable climate-Pw relationships in the Budyko framework. This may be an important reason ~~for the~~
109 ~~contradictory research results on the Pw~~ why there is disagreement among researchers about the factors and extent of
110 influence on Pw.

111 To fill the research gap. ~~The purpose of this study was to investigate what factors and effects relate to the Pw based~~
112 ~~on the proposed a~~ classification method of watersheds using the hydrologically similar groups ~~within the Budyko~~
113 ~~framework principle~~ and ~~develop~~ then developed a model framework for estimating the Pw (PwM) separately for different
114 watersheds in hydrologically similar groups to simulate global runoff. ~~We collected~~ We expect that classifying watersheds
115 into hydrologically similar groups is useful for exploring the effect of watershed characteristics on its water balance and
116 interpreting the physical meaning of the Pw in the Budyko framework. Overall, 726 records of hydrological data in 366
117 watersheds from globally published datasets ~~and were collected for analyses (Supplement 1). These 366 watersheds were~~
118 classified ~~these watersheds~~ into six hydrologically similar groups according to the hydrologically homogenous ~~regions~~
119 ~~applying attributes of watersheds using~~ the Decision Tree Regressor ~~to measured watershed attributes~~ method. Then, we
120 identified the controlling factors of the Pw from various environmental factors in each hydrologically similar group. ~~Based~~
121 ~~on the relationship between the Pw and its controlling factors, the PwM was set up by~~ and developed multiple non-linear
122 regression ~~methods~~ models for estimating the Pw in the Budyko framework. This study highlights the need to account for
123 the interactions among hydrologic, climatic, and watershed characteristic factors for explaining the Pw in the Budyko
124 framework.

125 **2.Fu's formula**

126 This study employed the Fu's formula (Zhou et al., 2015a) to analyze Pw in the Budyko framework. Among the
127 parametric equations, Fu's equation has received the most application and turned out to be a more generalized form (Zhou
128 et al., 2015a). The formula is expressed as:

$$129 \frac{R}{P} = \left(1 + \left(\frac{P}{PET} \right)^{-Pw} \right)^{\frac{1}{Pw}} - \left(\frac{P}{PET} \right)^{-1} \quad (1)$$

130 where R/P is a dimensionless annual water yield coefficient; P/PET is an aridity index; and Pw is a dimensionless constant
131 varying from 1 to infinity, and represents water retention capacity for evapotranspiration. When Pw=1, all the precipitation
132 would become flow and the residence time is 0. When Pw→infinity, all precipitation would remain in the watershed and
133 residence time would equal the time for all precipitation conversion to evapotranspiration. So, the natural watersheds with
134 a large Pw value may be “non-conservative” (i.e., precipitation is not the sum of streamflow and evapotranspiration),
135 because part of the water remain in the watershed may come from groundwater flow and other hardly or not measurable
136 flows. To be more cautious, in this study, the empirical upper limit for Pw was 10 to ensure that the watersheds in question
137 were conservative.

138 **2.3 Data**

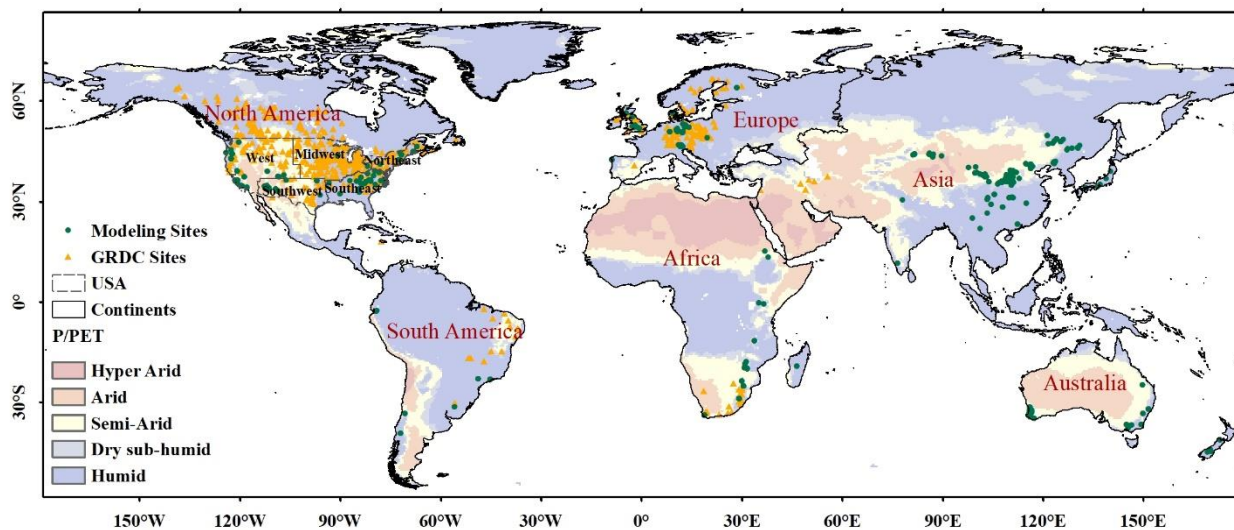
139 **2.3.1 Modeling Hydrological data**

140 ~~Global hydrological~~Hydrological data for modeling, including runoff (R, mm yr^{-1}) and corresponding precipitation
141 (PREP, mm yr^{-1}), were collected from globally published datasets (726 samples listed in ~~Supplementary Data~~Supplement
142 1, Fig. 1). Potential evapotranspiration (PET, mm yr^{-1}) data were downloaded from version 4.05 of the CRU TS (Climatic
143 Research Unit gridded Time Series) climate dataset (<https://doi.org/10.6084/m9.figshare.11980500>), which is produced by
144 the CRU at the University of East Anglia. For consistency, we used PET values extracted from the CRU TS dataset of all
145 watersheds listed in ~~Supplementary Data~~Supplement 1, even for studies with PET values reported. The PET values were
146 extracted based on the coordinate points of watersheds. Using collected and extracted the R, P and PET data, we calculated
147 the R/P and P/PET for each site. Then, we derived the Pw values according to Equation 1.

148 Observed river discharge data for validation were obtained from the Global Runoff Data Centre (GRDC,
149 https://www.bafg.de/GRDC/EN/02_srvcs/21_tmsrs/riverdischarge_node.html). Only the GRDC stations meeting the
150 following criteria were selected for further analysis: (1) The sites with continuous time-series runoff observations during

151 [the period 2000–2016 and corresponding surface soil moisture, fractional vegetation cover and seasonal index data were](#)
 152 [also available during such a period; \(2\) The drainage area reports can be found in the original data to provide area](#)
 153 [parameters for converting original flow volumes to runoff rates; \(3\) The geographical coordinates reports can be found in](#)
 154 [the original data and the shape of the drainage can be found in the GRDC Watershed Boundaries \(2011\); \(4\) The watersheds](#)
 155 [of “non-conservative” \(\$m>10\$ \) and unrealistic runoff rates \(\$m<1\$ \) are removed. Based on these criteria, 545 GRDC stations](#)
 156 [were selected for validation \(Fig. 1\). Then, the flow volumes of selected sites were converted to runoff rates \(Ghiggi et al.,](#)
 157 [2019\).](#)

158 [We used the boundary of watersheds provided by GRDC Watershed Boundaries \(2011\) to extract the average values](#)
 159 [of PET and P from grid datasets for each watershed. The PET values were extracted from the CRU TS dataset. The P values](#)
 160 [for runoff reconstruction were extracted from Global Precipitation Climatology Centre \(GPCC\) Precipitation Total Full](#)
 161 [V2018 \(0.5×0.5\) data provided by the NOAA/OAR/ESRL PSL, Boulder, Colorado, USA. It is because that the Global](#)
 162 [Precipitation Climatology Centre \(GPCC\) precipitation data was found to be more agreeable with the observation in the](#)
 163 [previous research compared to the CRU TS precipitation dataset\(Ahmed et al., 2019; Degefu et al., 2022; Fiedler and Döll,](#)
 164 [2007; Hu et al., 2018; Salaudeen et al., 2021\).](#)



165 **Figure 1.** Location of the observation sites for modeling (green dots) ($n = 726$) and the GRDC (Global Runoff Data Centre) observation
 166 sites (orange triangles) ($n = 545$) for validation. Background colors represent UNEP (1997) climate classification for P/PET values
 167 (Hyper Arid: $P/PET < 0.03$; Arid: $0.03 \leq P/PET < 0.2$; Semi-Arid: $0.2 \leq P/PET < 0.5$; Dry sub-humid: $0.5 \leq P/PET < 0.65$; Humid: $P/PET \geq 0.65$).
 168 The globe was divided into nine geographic regions: North America (west, southwest, midwest, northeast, southeast, except of the USA),
 169 South America, Africa, and Europe.

170

171

172 **3.2 Watershed characteristic-related data**

173 ~~The datasets of other watershed characteristic factors were extracted from remote sensing data. All datasets were~~
174 ~~aggregated at the same spatial resolution (0.5 degrees). The sources of datasets are summarized in Table 2.~~

175 The watershed characteristic-related factors mainly include surface soil moisture (0-10cm underground, SM),
176 fractional vegetation cover (FVC) and seasonal index (SI) of Walsh and Lawler (1981). For the GRDC watersheds, records
177 of these three fields were extracted from grid data based on the boundary files provided by GRDC Watershed Boundaries
178 (2011). For the collected watersheds from published literatures without boundary files, data of these three fields were
179 extracted from grid data according to the coordinate points of these watersheds. The sources of datasets are summarized in
180 Table 2.

181 **Table 2.** Data sources for watershed characteristic factors

Watershed characteristic factors	Data source/version	Units	Reference
Surface soil moisture (0-10cm underground, SM)	GLDAS Noah Land Surface Model L4	mm	Rodell et al. (2004)
Fractional vegetation cover (FVC)	GLASS FVC V4	m ² m ⁻²	Liang et al. (2021)
Seasonal index (SI)	CRU TS dataset version 4.03, global maps of seasonality indices	dimensionless	Walsh and Lawler (1981);Feng (2019)

182

183 **2.2 Validation data**

184 ~~Observed river discharge data for validation were obtained from the Global Runoff Data Centre (GRDC,~~
185 ~~https://www.bafg.de/GRDC/EN/02_srves/21_tmsrs/riverdischarge_node.html). The PET and PRE values corresponding to~~
186 ~~selected sites of GRDC were extracted from remote sensing data. PET values were extracted from the CRU TS dataset.~~
187 ~~PRE values were extracted from Global Precipitation Climatology Centre (GPCC) Precipitation Total Full V2018 (0.5×0.5)~~
188 ~~data provided by the NOAA/OAR/ESRL PSL, Boulder, Colorado, USA (https://psl.noaa.gov/data/gridded/data_gpcp.html).~~

189 **3.4 Methods**

190 **3.1 Budyko framework**

191 ~~This study employed the new Fu's formula (Zhou et al., 2015), a Budyko type equation derived from Fu's equation,~~
192 ~~to analyze Pw in the Budyko framework. Within the new Fu's model, the ratio (R/P) of annual water yield (R) to~~

193 precipitation (P) is determined by two variables: an aridity index (precipitation/potential evapotranspiration; P/PET), and
 194 $P_w(m)$. The formula is expressed as:

$$195 \frac{R}{P} = \left(1 + \left(\frac{P}{PET}\right)^{-m}\right)^{\frac{1}{m}} - \left(\frac{P}{PET}\right)^{-1} \quad (1)$$

196 where m is a dimensionless integration constant varying between 1 and infinity.

197 Based on the randomly selected 726 samples from global hydrological studies, we derived the $P_w(m)$ values for each
 198 sample.

199 3.24.1 Classification of watersheds into hydrologically similar groups using watershed attributes

200 A hydrologically similar group (hydrologically homogeneous region) is defined as a group of drainage basins whose
 201 hydrologic responses are similar (Kanishka and Eldho, 2020). Therefore, the relationship between P_w and [the watershed](#)
 202 [characteristic](#) variable does not change substantially in a hydrologically similar group. However, when that relationship
 203 between P_w and the variable changes as certain boundaries are crossed, the corresponding watersheds are divided into
 204 different groups by these boundaries.

205 Three watershed characteristic variables — [surface](#) soil moisture (SM), rainfall seasonality index (SI), and fractional
 206 vegetation cover (FVC) — were selected for classification. For SM and FVC, the bounded intervals of the variables were
 207 given by the Decision Tree Regressor (DTR). The locations of splits in DTR were used as dividing intervals. The Scikit-
 208 learn library (Pedregosa et al., 2011) in Python provides the DTR used in this study. [Based on The criterion for measuring](#)
 209 [the quality of the split was set to “poisson” which uses reduction in Poisson deviance to find splits. The “random” strategy](#)
 210 [was used to choose local optimal splitting at each node. The results and performances of DTR are shown in Supplement 2.](#)
 211 [Based on the criteria used by](#) Walsh and Lawler (1981), we divided the SI into three parts ($SI \leq 0.4$, $0.4 < SI \leq 0.8$, $SI > 0.8$) to
 212 represent three hydroclimatic ~~seasonalities~~ [seasonality](#) (precipitation spread throughout the year, marked seasonality with
 213 a short drier season, extreme seasonality with a long drier season). [Finally, six hydrologically similar groups were classified](#)
 214 [\(Table 3\).](#)

215 ~~Six hydrologically similar groups are detailed in Table 3.~~

216 **Table 3.** Classification of watersheds

Soil moisture classifier	Water soil regime	Seasonality index classifier	Seasonality precipitation regime	Fractional vegetation cover classifier	vegetation cover regime	Name of the group
SM \leq 20	Dry soil	—	—	—	—	IN _D

		SI ≤ 0.4	Seasonless	—	—	IN _{WP}
SM > 20	Wet soil	0.4 < SI ≤ 0.8	Marked seasonality	FVC ≤ 0.2 0.2 < FVC ≤ 0.5 FVC > 0.5	Low density Middle density High density	IN _{WMS} IN _{WMM} IN _{WML}
		SI > 0.8	Extreme seasonality	—		IN _{WE}

217 **3.4.2 Setup of proposed Pw simulation model (PwM)**

218 **4.2.1 PwM with the classification of hydrologically similar groups**

219 We performed regression analysis between the Pw and watershed characteristic variables to determine the [input](#)
220 [variables of the](#) PwM. The variables whose R² of the regression model was greater than 0.1 were selected as input variables.
221 ~~Then we~~ We used a polynomial as the basic model form. Each term of the polynomial depends on the regression model of
222 the corresponding variable and the Pw. For each hydrological group, the PwM is modeled as a function as:

223 ~~$m = \sum \beta_i \times f(x_i)$~~

224 $Pw = \sum Coef_n \times f(Var_n)$ (2)

225 where ~~m~~ Pw represents the value of the Pw; ~~x_i~~ Var_n represents the input ~~variables~~ [variable that pass the regression test](#); f
226 corresponds to the function derived from the regression of ~~m~~ Pw on ~~x_i~~ Var_n; ~~β_i~~ Coef_n represents the empirical coefficient
227 fitted by multiple non-linear regression (MNR).

228 **3.4.2.2 PwM without classification of hydrologically similar groups**

229 [For comparison, we estimated Pw without the hydrologically similar groups, defined as non_PwM. The non_PwM is](#)
230 [as follows.](#)

231 $non_Pw = a_1 \times SM^2 + a_2 \times SM + b_1 \times FVC^2 + b_2 \times FVC$ (3)

232 [where non_Pw is the annual value of Pw simulated by non_PwM; SM is annual average value of surface soil moisture \(0-](#)
233 [10cm underground\); FVC is annual average value of fractional vegetation cover; a₁, a₂, b₁ and b₂ represent the empirical](#)
234 [coefficient fitted by least square method.](#)

235 **3.4.3 Model validation**

236 **3.4.3.1 Performance metrics**

237 Three performance metrics were used to assess the accuracy of the PwM. The term N is the number of observations,
238 i is the ith value to be simulated, and y_s and y_o are the simulated and observed series, respectively.

239 The relative bias (RelBIAS) represents systematic errors. A positive ~~(negative)~~-value indicates a general
 240 overestimation ~~(, while a negative one indicates an~~ underestimation), ~~and the~~. The perfect agreement is achieved when
 241 RelBIAS ~~is equal~~ equals to zero. RelBIAS is defined as:

$$242 \text{RelBIAS} = \frac{\text{mean}(y_s - y_o)}{\text{mean}(y_o)} \quad (34)$$

243 The coefficient of determination (R^2) assesses ~~how strong~~ the linear relationship ~~is~~ between the simulated and ~~the~~
 244 observed time series data. ~~It is represented as a value between 0.0 and 1.0. The optimal value is 1 and indicates a perfect~~
 245 ~~fit~~. It is defined as:

$$246 R^2 = \left\{ \frac{\sum_{i=1}^N (y_o^i - \bar{y}_o)(y_s^i - \bar{y}_s)}{[\sum_{i=1}^N (y_o^i - \bar{y}_o)^2]^{0.5} [\sum_{i=1}^N (y_s^i - \bar{y}_s)^2]^{0.5}} \right\} \quad (4)$$

$$247 R^2 = \frac{\sum_{i=1}^N (y_o^i - \bar{y}_o)(y_s^i - \bar{y}_s)}{[\sum_{i=1}^N (y_o^i - \bar{y}_o)^2]^{0.5} [\sum_{i=1}^N (y_s^i - \bar{y}_s)^2]^{0.5}} \quad (5)$$

248 The Nash–Sutcliffe efficiency (NSE) (Nash and Sutcliffe, 1970), a goodness-of-fit index, is usually used to assess the
 249 accuracy of the model. When NSE = 1, the model predictions perfectly match the observed data. A value ~~lower~~ higher than
 250 0 indicates that the ~~observed~~ modeled mean is a ~~better~~ good predictor ~~than compared to~~ the ~~model~~ observed value. It is defined
 251 as:

$$252 \text{NSE} = 1 - \frac{\sum_{i=1}^N (y_s^i - y_o^i)^2}{\sum_{i=1}^N (y_o^i - \bar{y}_o)^2} \quad (56)$$

253 **3.4.24.3.2 Bootstrapping validation** Cross-validations using the bootstrap sampling method

254 We used cross-validation to test the stability of the proposed PwM using the bootstrap sampling method. The
 255 ~~available~~ collected public data were split into two parts, one for model training and ~~test sets~~ the other for ~~the purpose of~~
 256 ~~bootstrapping~~ model validation. A subset of 60% of the data was randomly selected ~~without replacement~~ using the bootstrap
 257 sampling method for training PwM. The ~~trained PwM was used to estimate the~~ remaining 40% of the ~~runoff data set, and~~
 258 ~~then the performance metrics were used to evaluate the difference between the estimated and observed values.~~ data was
 259 used to evaluate the model performance using the validation metrics in section 4.3.1. For each metric, the term N is the
 260 number of test sets, i is the ith value to be simulated by the trained PwM, and y_s and y_o are the simulated and observed series
 261 of test sets, respectively. The process was repeated randomly 10000 times. We documented the ~~model skill for each cross-~~
 262 validation result of each bootstrapping and showed them in ~~a~~ the violin plot (Fig. 3).

263 **3.4.3 4.3.3 Runoff Validations of GRDC time-series runoff reconstruction validation results**

264 **(1) The runoff reconstruction by using the PwM**

265 To assess the accuracy of the PwM, runoff reconstructions were generated using the Budyko framework in which the
266 value of Pw is derived from the PwM simulation.

267 **(2) Selection of GRDC stations and conversion of flow volumes to runoff rates**

268 To evaluate the estimates of runoff reconstructed by the PwM, only the GRDC stations meeting the following criteria
269 were selected for further analysis.

270 1) The timeseries has observations within the period 2000–2016 (when corresponding SM, FVC, and SI were
271 available).

272 2) The drainage area reports can be found in the original data. This criterion is designed to provide area parameters
273 for converting original flow volumes to runoff rates.

274 3) The geographical coordinates reports can be found in the original data and the shape of the drainage area can be
275 found in the GRDC Watershed Boundaries (2011). This choice was made to retrieve the geographic location of the station
276 and then extract the corresponding required values from remote sensing data.

277 4) Time series with unrealistic runoff rates are removed. It is generally agreed that in the Budyko framework, runoff
278 is maximum (minimum) when $m = 1$ (10). Observations out of range are considered unrealistic. This criterion has been
279 adopted to eliminate observations that are physically extremely unlikely.

280 Based on these criteria, 545 GRDC stations were selected for validation (Fig. 1).

281 Then, the flow volumes of selected sites were converted to runoff rates. The average year of catchment runoff can
282 equal the annual streamflow measured at the outlet divided by the watershed area, provided other water losses are minimal
283 (Ghiggi et al., 2019). Thus, runoff rates are obtained as:

284
$$R_{(GRDC)} = \frac{Discharge_{(GRDC)}}{Area_{(GRDC)}} \times \frac{1}{1000} \quad (6)$$

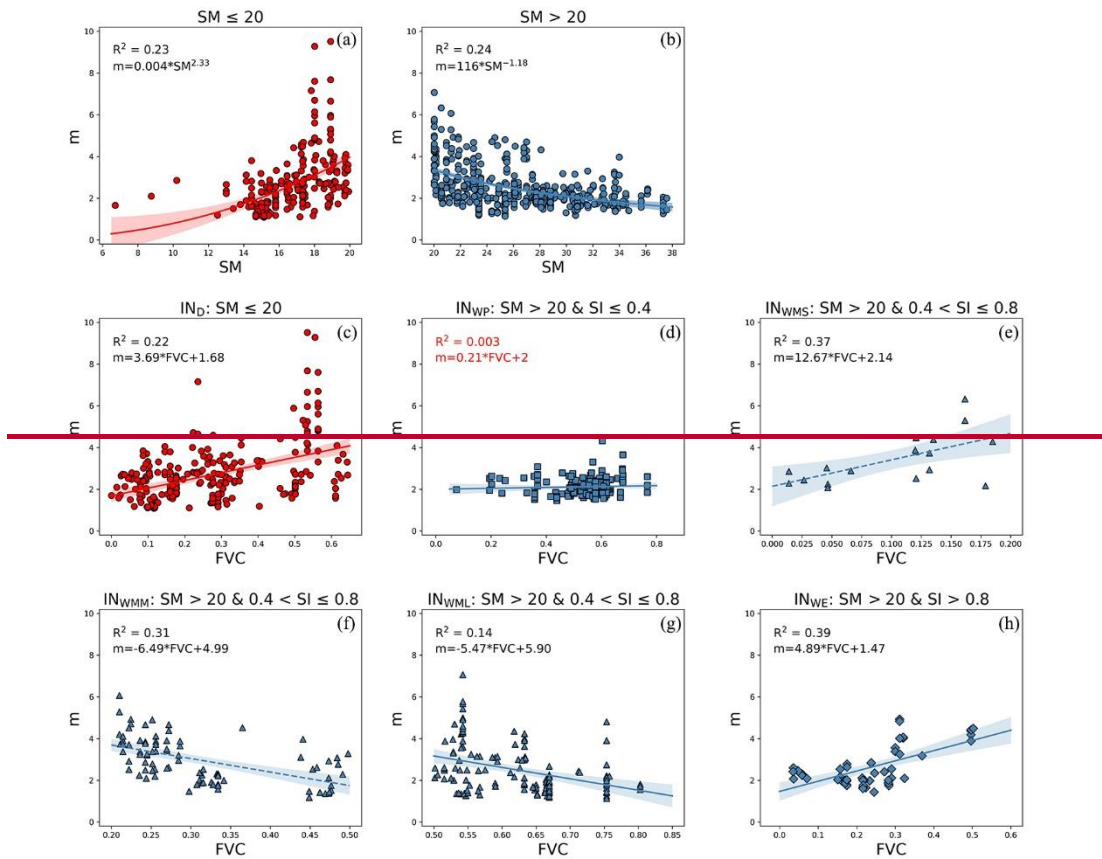
285 where $R_{(GRDC)}$ is the GRDC annual runoff rate (mm yr^{-1}); $Discharge_{(GRDC)}$ is the GRDC annual flow volume ($\text{m}^3 \text{yr}^{-1}$); $Area$
286 $_{(GRDC)}$ is the drainage area (km^2); 1000 is the conversion factor.

287 To further assess the model performance, we applied the proposed PwM into Fu's model to reconstruct the time-series
288 runoff data of GRDC from 2000 to 2016. Finally, the time-series runoff data from 545 GRDC stations, which were selected
289 by Sect. 3.1, were used to evaluate the model performance using the validation metrics in section 4.3.1. For each metric,
290 the terms y_s and y_o represent the simulated and observed time-series runoff data, respectively.

291 **45 Results**

292 **45.1 Model The new proposed model for estimating Pw in Fu's formula**

293 Figure 2 shows the results of the regression between m and watershed characteristic variables for the studied
 294 watersheds within new Fu's formula and helps assess the relationship between the Pw and watershed characteristic
 295 variables.



296
 297 **Figure 2.** Regression between m with (a-b) SM (soil moisture) and (c-h) FVC (fractional vegetation cover). Symbol colors represent
 298 dry (red) and wet (blue) soil moisture. Symbol shapes indicate seasonless (square), marked seasonality (triangle), and extreme seasonality
 299 (diamond). The equation in red indicates that the input parameter is rejected in the corresponding group. The groups are defined in Table
 300 3.

301 We found that the relationship between m and SM shows a positive power function for SM values from 0 to 20 (Fig.
 302 2a), while there is a negative power function with SM values from 20 to 100 (Fig. 2b). The relationship between m and
 303 FVC shows different situations in different groups (Fig. 2c-h). The relationship between m and FVC can be described as a
 304 positive linear equation in the IN_D group, the IN_{WSS} group, and the IN_{WE} group. The relationship can be described as a
 305 negative linear equation in the IN_{WMM} group and the IN_{WML} group. However, in the IN_{WP} group, the relationship between
 306 m and FVC is not significant. Therefore, FVC was rejected as the input variable in the IN_{WP} group.

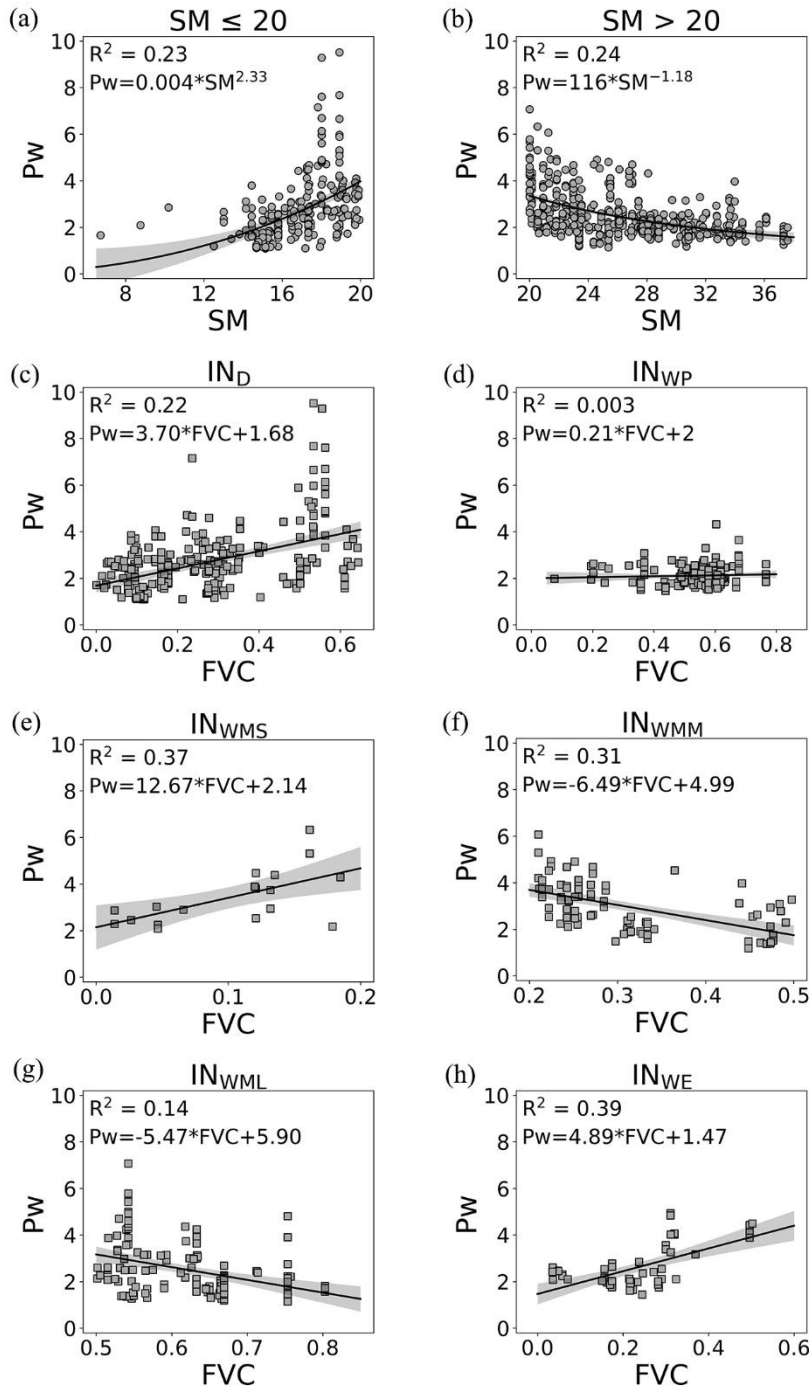
307 ~~Finally, the developed PwM is given by:~~

308 The regressions between Pw in Fu's formula and watershed characteristic variables collected from globally published
 309 datasets are shown in Fig. 2. Analyses show that soil moisture (SM) and fractional vegetation cover (FVC) are strongly
 310 correlated to Pw in each group. The Pw values in dry watersheds with SM<20mm monotonically increase with SM
 311 following a power function (Fig. 2a). However, in humid watersheds with SM>20mm, the Pw values convert to
 312 monotonically decrease with SM, which is also in a power function (Fig. 2b). And the fractional vegetation cover (FVC)
 313 shows linearly correlated with the Pw values of watersheds in most hydrologically similar groups but differ greatly between
 314 different groups (Fig. 2c-h). There is positive linear correlation between Pw and FVC in the IN_D, IN_{WMS} and IN_{WE} groups;
 315 while the relationship turns to be a negative linear equation in the IN_{WMM} and IN_{WML} groups. However, in the IN_{WP} group,
 316 the relationship between Pw and FVC is not significant. Therefore, in the proposed PwM, SM and FVC were selected as
 317 input variables (i.e., *Var. n*) for all the groups, except that FVC was rejected in the IN_{WP} group. The formula in PwM for
 318 calculating the Pw is modeled as sum of a power function of SM and a linear function of FVC, given by Equation 7.

$$\#Pw = \begin{cases} 0.91 \times SM^{0.38} + 1.48 \times FVC & (IN_D, SM \leq 20) \\ 28.72 \times SM^{-0.76} & (IN_{WP}, SM > 20, SI \leq 0.4) \\ 39.03 \times SM^{-0.96} + 11.82 \times FVC & (IN_{WMS}, SM > 20, 0.4 < SI \leq 0.8, FVC \leq 0.2) \\ 33.76 \times SM^{-0.71} - 1.47 \times FVC & (IN_{WMM}, SM > 20, 0.4 < SI \leq 0.8, 0.2 < FVC \leq 0.5) \\ 20.41 \times SM^{-0.42} - 4.221 \times FVC & (IN_{WML}, SM > 20, 0.4 < SI \leq 0.8, FVC > 0.5) \\ 3078 \times SM^{-2.43} + 3.53 \times FVC & (IN_{WE}, SM > 20, SI > 0.8) \end{cases} \quad (7)$$

320 where $\#Pw$ is the annual value of Pw; SM is annual average value of surface soil moisture ($kg \cdot m^{-2}$ 0-10cm underground);

321 FVC is annual average value of fractional vegetation cover ($m^2 \cdot m^{-2}$).



322

323

324

Figure 2. Regression between Pw in Fu's formula and (a) SM ($SM \leq 20$ mm), (b) SM ($SM > 20$ mm), (c) FVC (IN_D), (d) FVC (IN_{WP}), (e) FVC (IN_{WMS}), (f) FVC (IN_{WMM}), (g) FVC (IN_{WML}), and (h) FVC (IN_{WE}). Symbol shapes indicate SM (dot) and FVC (square).

325

4.2 Model validation 5.2 Cross-validations based on data collected from globally published literatures

326

Figure 3 helps evaluate the performance of PwM by showing the results of the global bootstrapping validation. Overall,

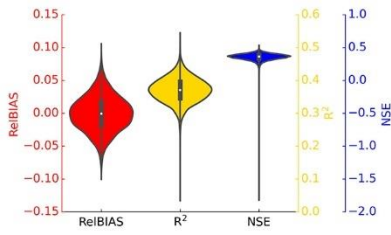
327

the PwM performs well, as indicated by satisfactory skill scores (Fig. 3a). The performance of the PwM and non_PwM

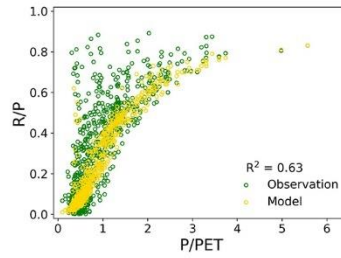
328 were cross-validated based on the data collected from globally published literatures using the bootstrap sampling method
329 (Fig. 3).

330 On average, the ensemble RelBIAS of the ~~non~~Pw simulated by the ~~model~~PwM is slightly negative (Fig. 3a), indicating
331 a weak tendency to underestimate the values of Pw, but the maximum relative bias is less than 0.1. The interquartile range
332 of R^2 for the PwM is from 0.35 to 0.40, with a median of 0.37. The scores of R^2 are higher than 0.3 in more than 95% of
333 the ~~global bootstrapping~~ bootstrap sampling events. The ~~global~~NSE skill scores show that in most ~~bootstrapping~~
334 ~~events~~bootstrap samplings, the estimation error estimated variance for the PwM is less than the variance of the observations
335 ($NSE > 0$), with the interquartile range from 0.33 to 0.39. In comparison, the maximum relative bias of the Pw simulated
336 by the non_PwM is 0.12, the median of R^2 is 0.13, and the median of NSE is 0.13. Overall, cross-validations show that the
337 performance of the PwM with the hydrologically similar groups is better and more stable than that of the non_PwM. Figure
338 ~~3b compares the published R/P observations against those simulated by the PwM. The R^2 between the observed and the~~
339 ~~simulated values is higher than 0.63. The model performs well in arid and semi-arid regions. The main underestimated~~
340 ~~regions are the dry sub-humid regions and humid regions with Aridity Index values less than 1. In terms of the distribution~~
341 ~~of simulated and observed differences (Fig. 3c), the global R/P simulations are dominated by weak underestimations, of~~
342 ~~which larger underestimations occurred in western America and northwest China.~~

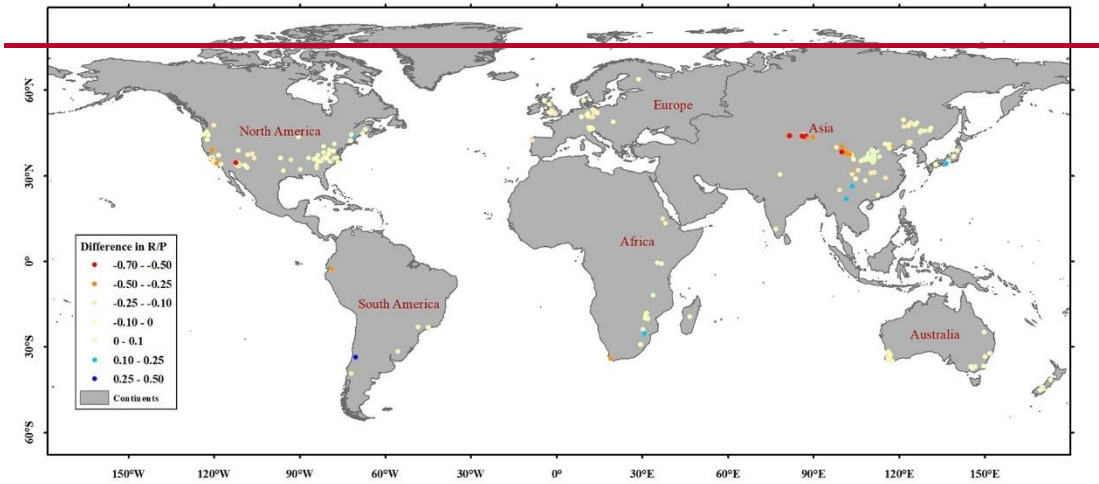
(a) Accuracy evaluation of PwM at bootstrapped data for global



(b) Scatterplot of R/P against P/PET



(c) Difference between the model and the observation R/P



343

344

345

346

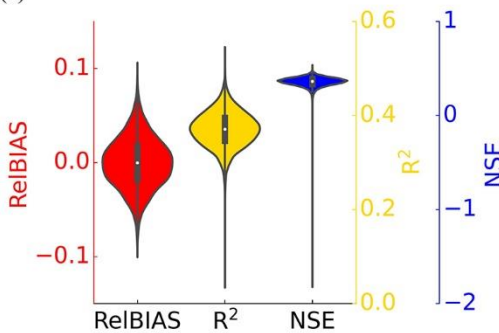
347

348

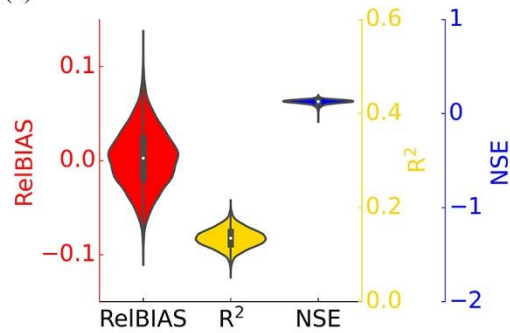
Figure 3. Global accuracy evaluation of the PwM. (a) Violin plot of skill scores for global bootstrapping. A violin represents the distribution of the considered skill scores of the bootstrapping validation. The white dot on the violin plot represents the median. The black bar in the center of the violin represents the interquartile range. Colors distinguish three performance metrics: Red (RelBIAS), yellow (R²) and blue (NSE). (b) Scatter plots between the R/P simulated by PwM and P/PET (yellow) and those from published data and P/PET (green). (c) Difference between the R/P values from the PwM and the published observations.

349

(a)



(b)



350

351

352

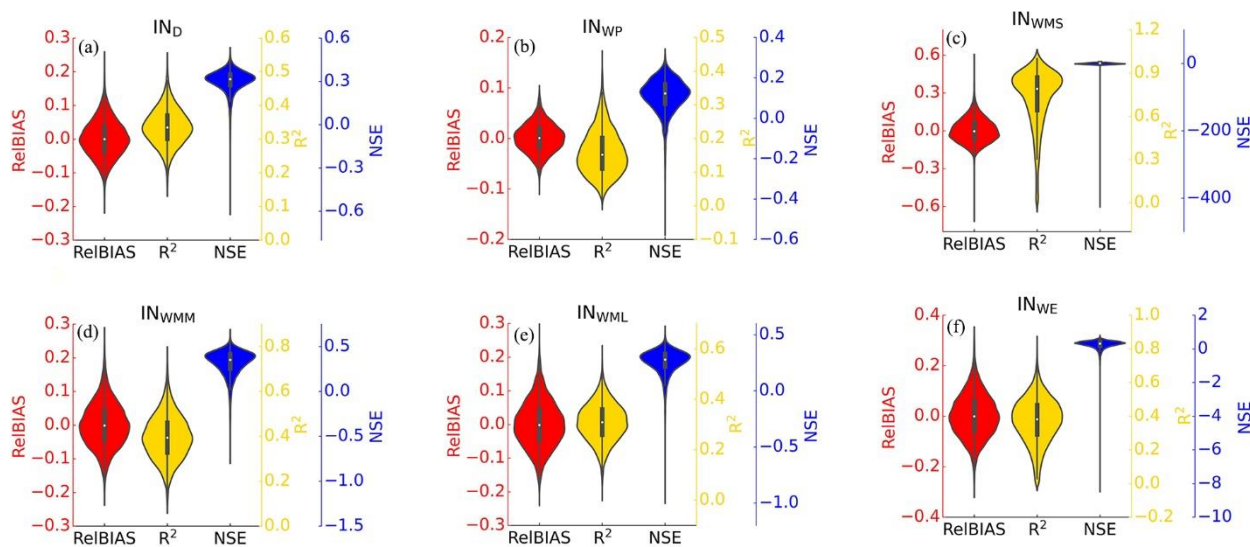
353

354

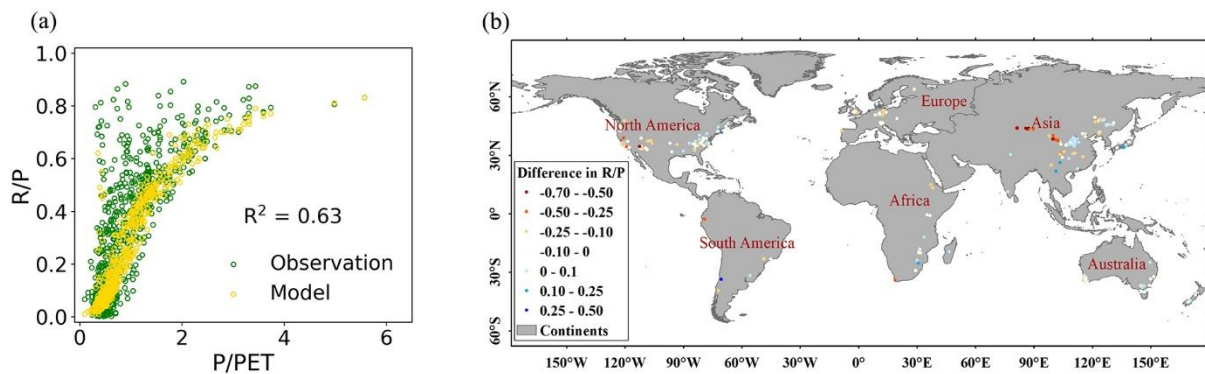
Figure 3. Cross-validation results of (a) PwM and (b) non_PwM. A violin represents the distribution of the considered skill scores. The white dot on the violin plot represents the median. The black bar in the center of the violin represents the interquartile range. Colors distinguish three performance metrics: Red (RelBIAS), yellow (R²) and blue (NSE).

355 The skill scores of cross-validations for the six intervals groups are shown in (Fig. 4) ~~show more variability,~~
 356 respectively. Though the overall RelBIAS of the PwM is negative, the PwM tends to overestimate values of Pw in the IN_{WP}
 357 group (the median of RelBIAS is positive). ~~R² scores vary widely between groups.~~ The IN_{WMS} group scores highest in R²,
 358 with a median of 0.73, and the lowest in the IN_{WP} group with a median of 0.16. The grouped NSE scores show more
 359 uncertainty than the overall, especially in the IN_{WMS}, ~~although the value of:~~ the lower adjacent value (LAV) larger than
 360 zero indicates more skill than the mean of observations, ~~and~~ however, the outliers are far below zero. The low NSE value
 361 may be due to the low number of watersheds sampled in this interval, which increased the inconclusive results.

362 Figure 5 showed the simulated R/P by the PwM in compassion to site observations. The R² between the observed and
 363 the simulated values is 0.63 (Fig. 5a). The model performs well in humid regions with P/PET>1 at southeast America,
 364 Europe, middle China and southeast of Australia. However, the PwM likely underestimated the runoff in the arid
 365 (P/PET<0.2) and semi-arid regions (0.2<P/PET<0.5), which mainly occurred in western America and northwest China (Fig.
 366 5b).



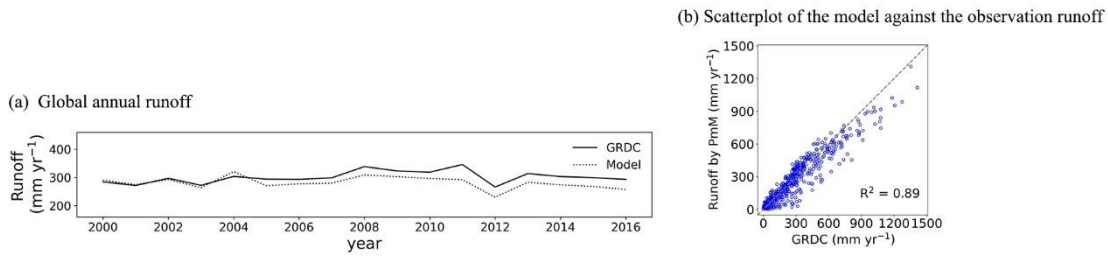
367 **Figure 4. Accuracy evaluation** Cross-validation results of PwM ~~at bootstrapped works~~ for (a) IN_D, (b) IN_{WP}, (c) IN_{WMS}, (d) IN_{WMM}, (e)
 368 IN_{WML}, and (f) IN_{WE}.
 369



370
 371 **Figure 5.** Simulated R/P using PwM in comparison with the observations collected from published literatures. (a) Scatter plots
 372 between R/P (yellow: simulation; green: observations) and P/PET; (b) Difference between simulated R/P from the PwM and
 373 observations from the published datasets.

374 **4.3 Runoff reconstruction validation** **5.3 Validations of reconstructing the time-series GRDC runoff**

375 ~~The runoff reconstruction results are shown in Fig. 5. The global~~ For the selected 545 GRDC watersheds, the
 376 annual runoff estimated by the PwM ranges from 229.84 to 320.34 mm, which is slightly lower than the observed
 377 range of GRDC (265.82 ~ 345.50 mm yr⁻¹) (Fig. 5a6a). Overall, the temporal evolution of runoff is captured well in
 378 the period 2000-2010. However, since 2011, the consistency between reconstructed runoff and GRDC runoff ~~has~~
 379 ~~decreased~~ ~~decreases~~, and the reconstruction results are constantly lower than the GRDC observations. ~~Influenced by~~
 380 ~~the underestimations in 2011-2016, the~~ The scatter plot between simulated and observed R/P also shows a slight
 381 ~~underestimation of~~ reconstructed global long-term mean runoff ~~also shows a slight underestimation~~ (Fig. 5b6b). The
 382 spatial patterns of long-term mean runoff ~~reconstruction~~ are shown in Fig. 5e6c-f. The ~~global~~ estimated ~~time-series~~
 383 runoff shows lower values in the west of the United States and south of Africa, and ~~show~~ higher values in the
 384 northeastern United States and the European Mediterranean area. ~~Overall, the reconstructed spatial patterns are~~
 385 ~~compatible, in comparison~~ with ~~other reported findings (Ghiggi et al., 2019)~~ ~~the GRDC time-series.~~



386

387

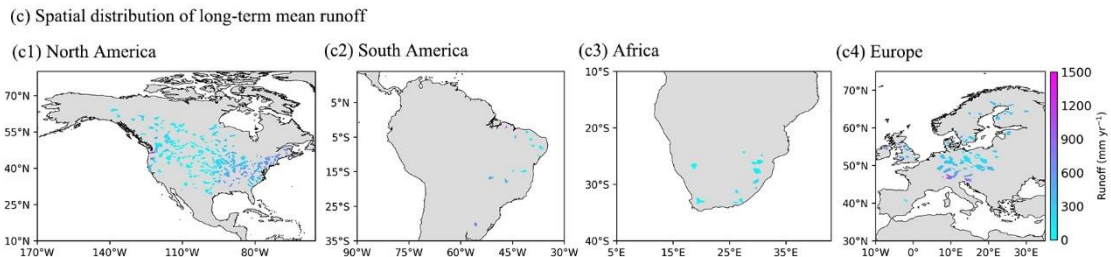
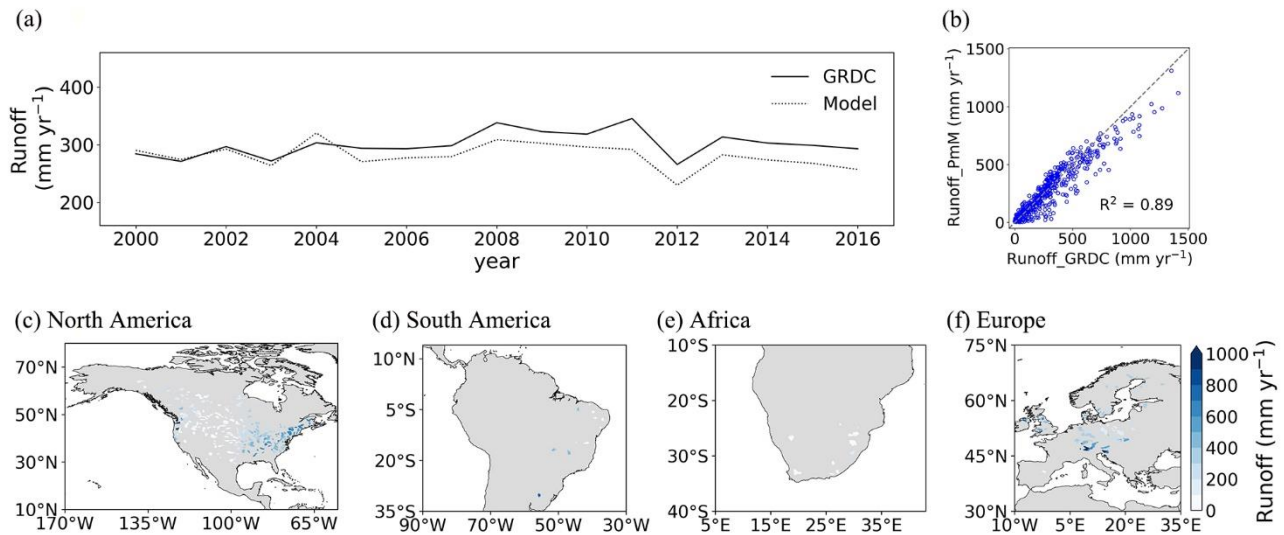


Figure 5. Runoff reconstruction results based on selected GRDC stations.



388

389

390

391

392

393

394

395

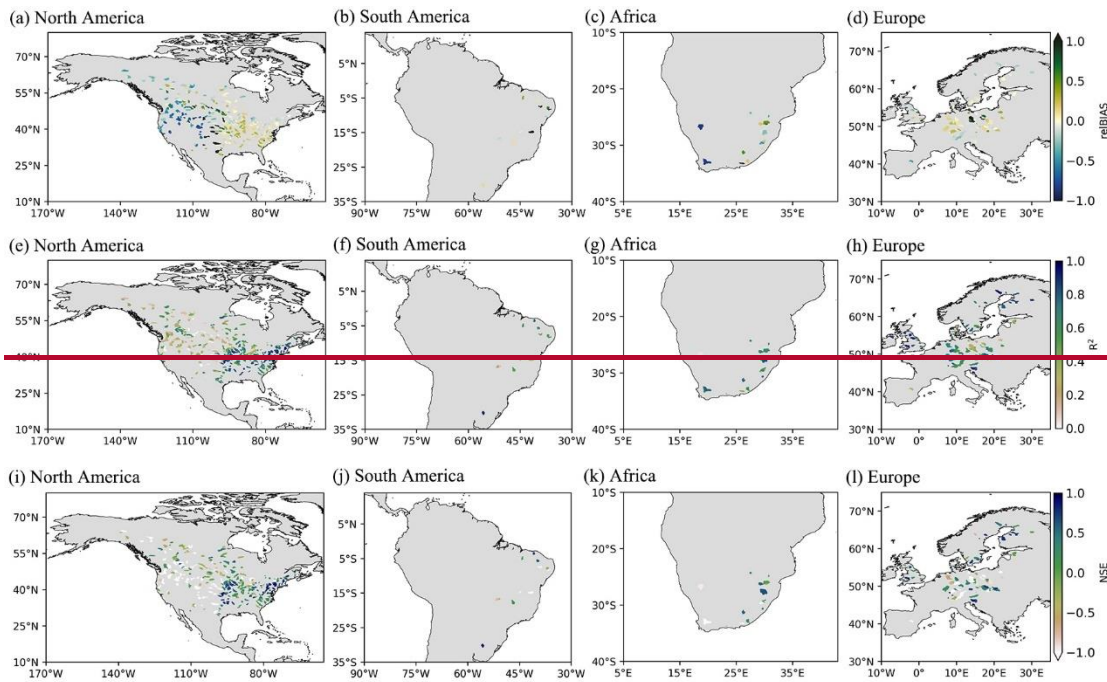
396

397

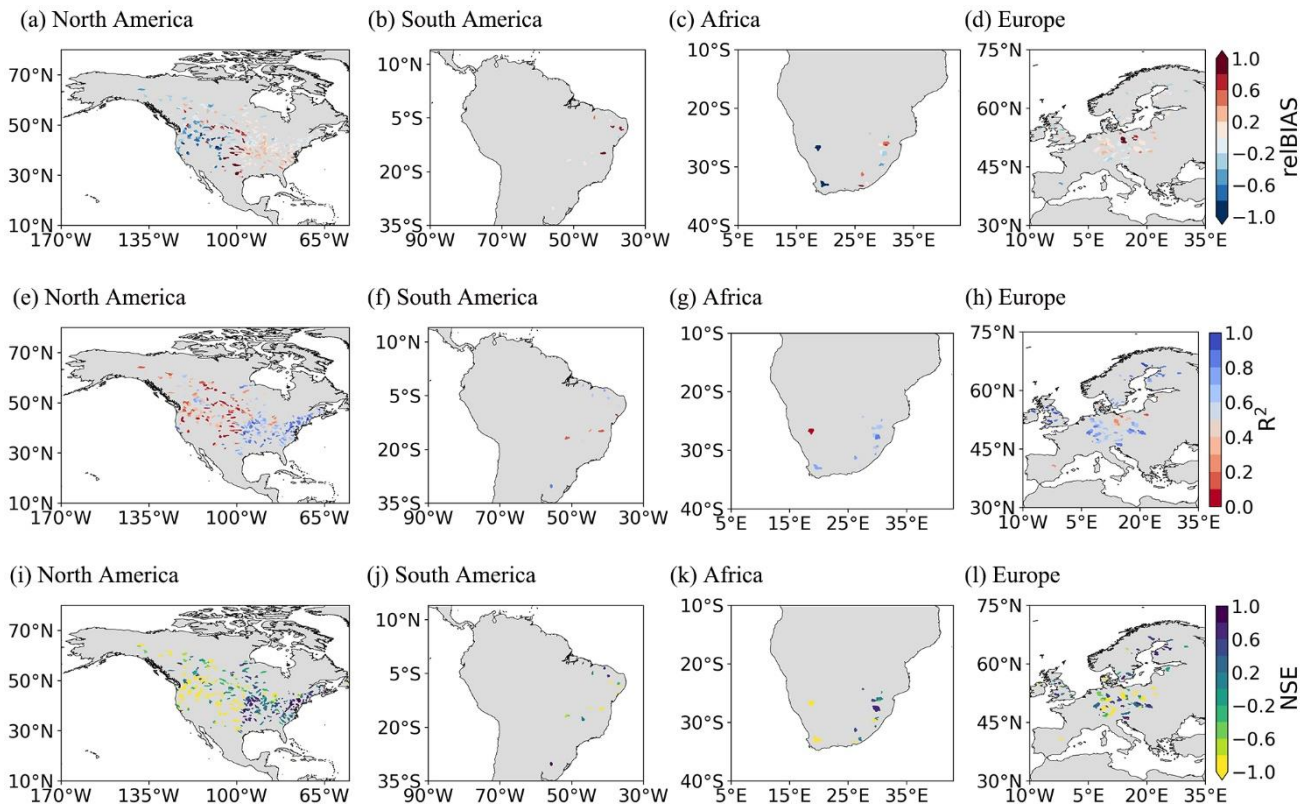
Figure 6. Time-series runoff reconstruction results in the selected GRDC stations. (a) Time-series annual mean runoff of the selected 545 GRDC watersheds; (b) Scatterplot between the modeled runoff and observed runoff. The spatial distribution of annual mean runoff in (c) North America, (d) South America, (e) Africa, and (f) Europe.

Figure 7 displays the considered-skill scores of the reconstructed runoff obtained from each watershed of by the selected PwM in comparison with the GRDC ensemble from 2000-2016. It can be seen that the result of reconstruction with by PwM, in general, is satisfactory, as indicated by the RelBIAS close to 0. The main area of underestimation is of runoff mainly occurs in the high mountains of the western United States (Fig. 7a), when the runoff is much smaller. In the lower part of the runoff rate distribution, the runoff tends to be underestimated. Humid regions such as the northeastern

398 United States and the European Mediterranean area have quite high R^2 values, while lower values are observed in [the](#) semi-
 399 arid ($0.2 < P/PET < 0.5$) and [the](#) dry sub-humid ($0.5 < P/PET < 0.65$) regions, which are mainly ~~found~~ [located](#) in the western
 400 and midwestern United States ([Fig. 7e-h](#)). ~~The~~ [There is](#) low NSE scores ~~tend to correspond to~~ [in](#) the watersheds where
 401 runoff is unusually under-[estimated](#) or over-estimated ([Fig. 7i-l](#)). ~~Especially, the model performance indicated by NSE~~
 402 ~~decreases when runoff is underestimated especially~~ [decreases](#) in the western United States.



403



404

405 **Figure 67.** Spatial distribution of the skill scores of the reconstructed [time-series](#) runoff.

406

407

408

409

410

411

412

413

414

415

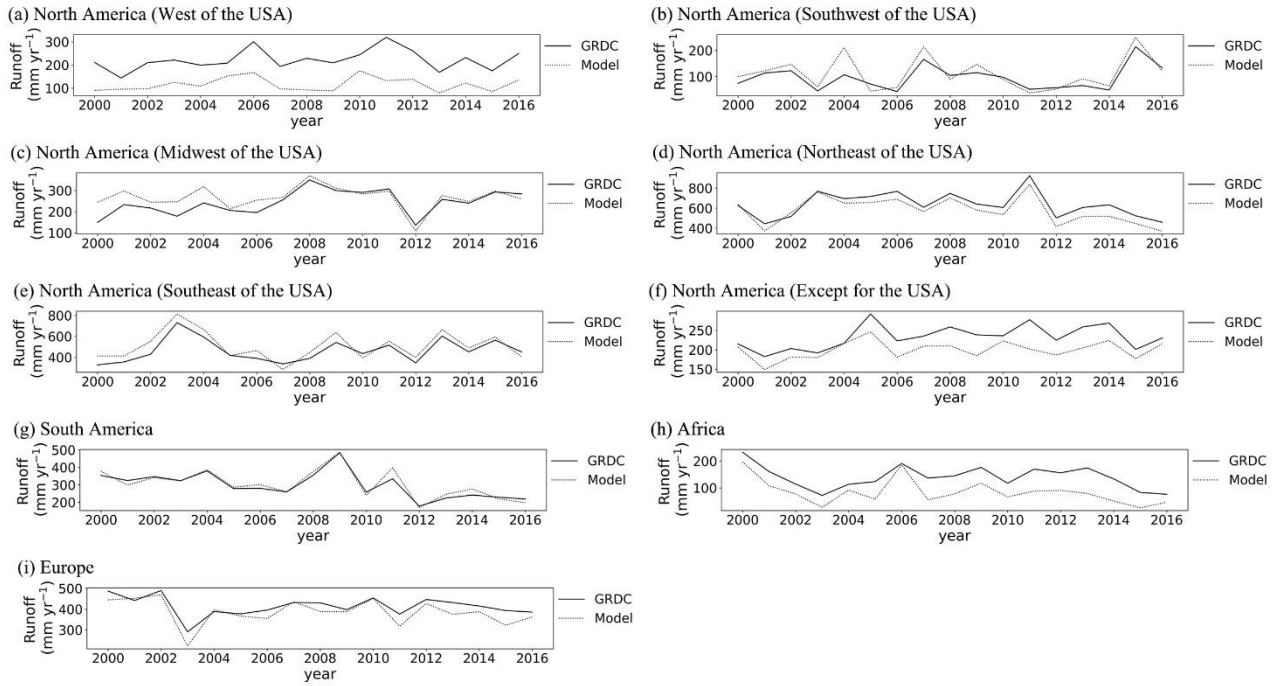
416

417

418

419

We ~~divided~~[classified](#) the ~~world~~[GRDC data](#) into nine geographic regions (Fig. 1) ~~to~~[and](#) further ~~evaluate~~[evaluated](#) the performance of PwM ~~on a global scale~~ in each sub-region individually. ~~Figure 7 shows the observational agreement of runoff time series and long term mean for nine geographic regions. The temporal evolution of runoff is,~~ In general, ~~well captured,~~ the simulated time-series runoff is consistent with the time-series observations (Fig. 8-9), except in the western United States, where runoff was consistently underestimated (Fig. 8a). ~~In addition, the runoff estimated by PwM~~ Spatially, there is ~~underestimated~~[an underestimation of runoff](#) in 2011 ~~to a greater extent than in other years. The regions where runoff was underestimated include sub-regions like~~ the western United States (Fig. 8a) and high latitudes in North America, ~~and the~~ (Fig. 8f). The runoff underestimation is more severe in the arid ~~areas in the~~ western United States (Fig. 9a) than in the relatively wet ~~areas in the~~ northwest of North America (Fig. 9f). ~~We considered that glacial meltwater might be the main cause of runoff underestimation. The reconstructed time-series runoff in the Milk River watershed (GRDC station number: 4220501) and Near Lethbridge watershed (GRDC station number: 4213111) both show an underestimation of annual runoff in the arid areas. The Milk River and the Near Lethbridge are two adjacent watersheds with similar drainage areas located on the border of the United States and Canada. However, the underestimation is more serious in Milk River watershed (RelBIAS=-0.32, annual mean P/PET=0.52) than in the Near Lethbridge watershed (RelBIAS=-0.27, annual~~



434

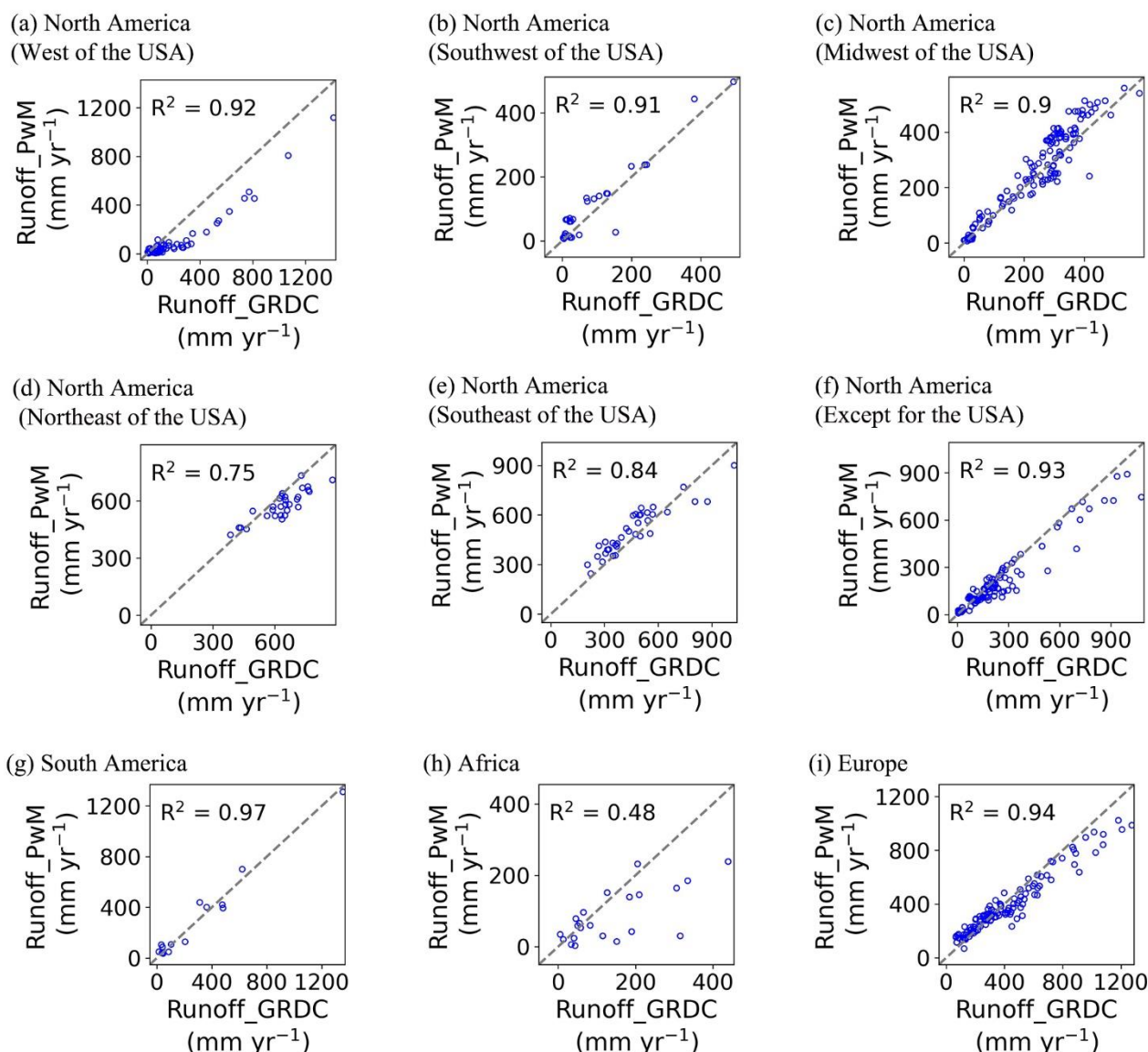
435

436

437

438

Figure 8. Observed time-series runoff versus reconstructed time-series runoff. Nine geographic sub-regions were in Fig. 1: North America ((a) west, (b) southwest, (c) midwest, (d) northeast, (e) southeast, (f) except of the USA), (g) South America, (h) Africa, and (i) Europe.



439
 440 [Figure 9. Scatterplots between observed annual mean runoff and reconstructed annual mean runoff. Nine geographic sub-regions were](#)
 441 [in Fig. 1: North America \(\(a\) west, \(b\) southwest, \(c\) midwest, \(d\) northeast, \(e\) southeast, \(f\) except of the USA\), \(g\) South America,](#)
 442 [\(h\) Africa, and \(i\) Europe.](#)

443 **56 Discussion**

444 Zhou et al. (2015a) provided a Budyko equation derived from Fu's equation and confirmed that this is a valid
 445 framework for studying hydrological responses. However, the physical meaning of ~~parameter m , a the~~ Pw in the Budyko
 446 equation, has remained unknown (Greve et al., 2015; Reaver et al., 2022; Zhou et al., 2015b; Zhang et al., 2004). In this
 447 paper, we selected the new Fu's equation and developed ~~PwM, a universal framework for estimating Pw, and exploring its~~
 448 ~~physical meaning. The Our~~ results show that, to a large extent, ~~PwM can estimate the Pw with in Budyko equation can be~~

449 ~~well estimated by the PwM using only~~ soil moisture and fractional vegetation ~~cover parameters~~. ~~As important hydrological~~
450 ~~watershed characteristics~~, ~~This indicates that~~ soil moisture and fractional vegetation cover strongly control the ~~Pw and~~
451 ~~affect runoff by the Budyko framework~~ ~~water balance of watersheds~~ (Gan et al., 2021; Chen and Sivapalan, 2020; Yang et
452 ~~al., 2009; Wang et al., 2021~~).

453 ~~The universal framework PwM~~ ~~The new proposed framework~~ for ~~calculating~~ ~~derivation of~~ the Pw ~~presented~~ in the
454 ~~paper Budyko equation~~ is built on empirically-based power ~~relationships between Pw and~~ ~~function of~~ soil moisture and a
455 ~~linear relationships between Pw and fractional vegetation cover~~ ~~function of fractional vegetation cover~~ (Equation 7).
456 ~~Concerning~~ ~~Our findings are consistent with those of Chen and Sivapalan (2020), which also indicated~~ the power relationship
457 between Pw and soil moisture, ~~our findings seem to confirm those of Chen and Sivapalan (2020)~~. However, the observed
458 ~~power relationship showed an evident~~. The important finding here is that there is a critical soil moisture threshold at 20
459 ~~mm~~ (Fig.2) to classify the watersheds with two different water balances. The Pw values in dry watersheds ($SM < 20\text{mm}$)
460 ~~monotonically increases with SM~~ but in humid watersheds ($SM > 20\text{mm}$) converts to monotonically decrease with SM. in
461 ~~power functions~~ — a positive power function appeared in the interval of 0 to 20 kg m^{-2} (Fig. 2a), while a negative power
462 ~~function was more appropriate from 20 to 100 kg m^{-2}~~ (Fig. 2b). The ~~possible-probable~~ reason for the threshold may be is
463 that transpiration ~~increased usually increases~~ as ~~the relative extractable~~ soil water ~~increased until reaching a~~ ~~increases in a~~
464 ~~relative dry condition~~ (Jiao et al., 2019; Bierhuizen, 1958; Wang et al., 2012; Yao et al., 2016; Schwarzel et al., 2020).
465 ~~However, once the~~ soil moisture ~~exceeds the~~ threshold ~~value~~. ~~Once the soil moisture threshold was exceeded, like 20 mm~~
466 ~~in this study~~, the acceleration of transpiration from soil moisture ~~slowed-slows~~ down, ~~and excess soil moisture provided~~
467 ~~conditions for high runoff ratios~~ quickly (Havranek and Benecke, 1978; Verhoef and Egea, 2014; Metselaar and De Jong
468 ~~Van Lier, 2007~~). These findings are ~~largely-highly~~ in line with previous studies (Havranek and Benecke, 1978; Jiao et al.,
469 2019; Cavanaugh et al., 2011; Ducharme et al., 1998), although the threshold of soil moisture varied ~~in~~ ~~slightly~~ between
470 these studies, ~~(e.g., the results of Ducharme, Cavanaugh and Jiao show that the threshold value is 0.25, 0.10 and 0.20 $\text{m}^3 \text{m}^{-3}$~~
471 ~~, respectively)~~ e.g., 0.25 $\text{m}^3 \text{m}^{-3}$ in Ducharme et al. (1998), 0.10 $\text{m}^3 \text{m}^{-3}$ in Cavanaugh et al. (2011) and 0.20 $\text{m}^3 \text{m}^{-3}$ in Jiao
472 ~~et al. (2019), respectively~~.

473 ~~Our study found a close linear relationship between Pw and fractional vegetation cover, and a similar linear~~
474 ~~relationship has been reported in previous studies~~. This study confirms a close linear relationship between Pw and fractional
475 ~~vegetation cover, similar as those reported in previous studies~~ (Ning et al., 2017; Zhang et al., 2018; Xu et al., 2013). For
476 example, Li et al. (2013) found that the spatial pattern of the Pw was linearly correlated with the spatial pattern of the

477 vegetation cover fraction. However, ~~these reports were mostly from studies in large watersheds or non-humid watersheds.~~
478 ~~At the global scale, including small and wet watersheds, vegetation was considered~~ previous similar findings were mostly
479 reported in large watersheds or non-humid watersheds (Li et al., 2013; Gan et al., 2021). For those small and wet watersheds,
480 vegetation-related factors were considered to be weakly correlated with the watershed characteristic parameter of the
481 Budyko framework (Liu et al., 2021; Padrón et al., 2017; Yang et al., 2014). ~~The classification of watersheds might provide~~
482 ~~some insights for explaining this paradox. The findings in this paper show that there were different relationships between~~
483 ~~fractional vegetation cover and Pw in different hydrological similarity groups.~~ The classifications of watersheds into
484 different hydrological similarity groups in this study provide new insights for explaining this confusion. In dry ~~soil~~
485 watersheds (IN_D), the relationship between Pw and fractional vegetation cover followed a positive linear function (Fig. 2c).
486 This finding was consistent with the majority view that vegetation transpiration increases (reflected by the increased Pw)
487 with increasing vegetation coverage in regions with insufficient soil moisture (Wang et al., 2012; Yao et al., 2016;
488 Schwarzel et al., 2020). In wet ~~soil~~ watersheds, ~~the relationship between vegetation and Pw also depends on the seasonality~~
489 ~~of precipitation and the size of vegetation: the relationship between the Pw and FVC could be described as a positive linear~~
490 ~~equation in the IN_{WSS} and the IN_{WE} groups.~~ In contrast, a negative linear equation is needed in the IN_{WMM} and IN_{WML}
491 groups: the relationship between Pw and fractional vegetation cover is not only affected by the SI seasonality, but is also
492 restricted by the background value of fractional vegetation cover itself. This is typical obvious in wet watersheds with
493 marked SI seasonality ($0.4 < SI < 0.8$). Despite having similar seasonal conditions, the Pw values in the watersheds with low-
494 density vegetation coverage ($FVC < 0.2$) monotonically increase with FVC (Fig. 2e). However, the Pw values in the
495 watersheds with middle-density ($0.2 < FVC < 0.5$, Fig. 2f) and the high-density ($FVC > 0.5$, Fig. 2g) vegetation coverage
496 monotonically decrease with FVC. This confirms that climate, soil moisture, and vegetation coverage are not independent
497 factors affecting the water balance, and the physiological characteristics of vegetation greatly depend on climate and soil
498 moisture (Gan et al., 2021; Yang et al., 2009). When vegetation was coupled with other catchment properties, the watershed
499 characteristic parameter exhibited greater variations (Gan et al., 2021). Therefore, the classification of watersheds is crucial
500 and supports the hypothesis that watersheds in the same class would function in a similarly in environments with similar
501 climate, soil moisture, and vegetation environment characteristics (Kanishka and Eldho, 2017; Sinha et al., 2019). ~~The~~
502 ~~relationship between watershed characteristic variables and Pw may be confused without watershed classification.~~

503 Although ~~the validation showed that~~ the overall performance of PwM was satisfactory, we noted that the accuracy of
504 the runoff simulated by the Budyko framework in some regions ~~was likely not optimal~~ show either an overestimation or

505 ~~an underestimation. Because It is because~~ the Pw ~~was in our study is~~ only forced with soil moisture, seasonality index and
506 fractional vegetation cover, ~~and thus~~ the estimated runoff could not clearly account for ~~impacts from other drivers, like~~ the
507 effects of temperature anomalies and ~~excess~~ glacial meltwater on the hydrological regimes (Liu et al., 2022b). This ~~may~~
508 ~~be is probably~~ one of the ~~main~~ reasons for the severe underestimation of runoff in western North America and southern
509 Europe (Fig. 7a, d). ~~The time-series and spatial distribution results of runoff validation also point to these reasons. However,~~
510 ~~the spatial resolution of the considered remote sensing data did not allow to capture the variability of snowmelt volume~~
511 ~~governed by the unusually high temperatures. Perhaps future research could examine the relationship between watershed~~
512 ~~characteristic parameters and glacier melting caused by temperature anomalies and further improve the accuracy of runoff~~
513 ~~simulation based on the Budyko framework. Future in-depth researches are in need to examine influences from other impact~~
514 ~~factors to improve the accuracy of Pw estimation in the Budyko framework.~~

515 **67 Conclusions**

516 This ~~research study~~ developed PwM, a ~~universal model new~~ framework for estimating the Pw ~~and exploring its~~
517 ~~physical meaning in the Budyko framework for watersheds in similar environments based on the hydrologically similar~~
518 ~~groups principle. The development of PwM using~~ Generally, the proposed method not only represented the runoff
519 ~~observations in 366 watersheds from~~ global hydrological data collected from globally published datasets and validated
520 ~~using literatures, but could also reconstruct the time-series runoff in 545~~ GRDC ~~observational data provides confidence in~~
521 ~~PwM. The results show that the overall performance of PwM is satisfactory~~ stations. Moreover, the findings indicated that
522 the Pw is closely related to soil moisture and fractional vegetation cover, and the relationship varies across specific
523 hydrologic similarity groups. ~~However, due to the complexity of hydrological processes, the new framework could not~~
524 ~~fully account for the impacts from all other factors, which might result in an underestimation of runoff in regions with~~
525 ~~glaciers or under climate with temperature anomalies. Overall, our findings lay a sound basis for estimating the Pw in the~~
526 ~~Budyko framework, provide references for calibrating the hydrological models, and will be helpful for improving global~~
527 ~~runoff estimations.~~

528 ~~Due to the complexity of hydrological processes, the PwM could not fully account for all the dynamic impacts of~~
529 ~~watershed characteristics, such as temperature anomalies and excess glacial meltwater, which might result in an~~
530 ~~underestimation of runoff in regions with glaciers. Therefore, the interactions of climate and glaciers should be explicitly~~

531 ~~incorporated into a future Budyko framework. To achieve this, detailed hydrological and glacial melt datasets at fine spatial~~
532 ~~and temporal scales are also needed.~~

533 ~~The positive findings lay a sound basis for explaining the Pw in the Budyko framework. They could also be applied~~
534 ~~to improve global runoff estimations. We hope it will improve water balance estimates, pave the way for future hydrology~~
535 ~~research, and help consolidate water resources management studies.~~

536

537 *Code availability.* The pieces of code that were used for all analyses are available from the authors upon request.

538 *Data availability.* All data used in this study are publicly available. PET data are available from CRU TS
539 (<https://doi.org/10.6084/m9.figshare.11980500>), SM data are available from GLDAS
540 (https://disc.gsfc.nasa.gov/datasets/GLDAS_NOAH025_M_2.1/summary?keywords=GLDAS), FVC data are available
541 from GLASS (<http://www.glass.umd.edu/05D/FVC/>), SI data are available from HydroShare
542 (<http://www.hydroshare.org/resource/ff287c90c9e947a78e351c8d07d9d3f3>), ~~PRE-P~~ data used to model validation are
543 available from GPCC (<https://psl.noaa.gov/data/gridded/data.gpcc.html>), and observed river discharge data are available
544 from GRDC (https://www.bafg.de/GRDC/EN/02_srvcs/21_tmsrs/riverdischarge_node.html).

545 *Author contributions.* ~~YC and~~ XC designed the study and proposed the scientific hypothesis. YC implemented the
546 experiments, conducted the analysis and wrote the paper. MX helped with data collection, and checked the technical
547 adequacy of the experiments. CY and WZ helped with data processing. [WPY provided the guidance on the seasonal indices](#)
548 [\(SI\)](#). CY, WZ, CJ, ~~and WY~~ [WY, WTY and WPY](#) reviewed and edited the manuscript. XC oversaw the study and conducted
549 manuscript revision as a mentor.

550 *Competing interests.* The contact author has declared that neither they nor their co-authors have any competing interests.

551 *Financial support.* This study was financed by the National Natural Science Foundation of China (grant numbers 31971458,
552 41971275), Innovation Group Project of Southern Marine Science and Engineering Guangdong Laboratory (Zhuhai), grant
553 number 311021009 and the Special High-level Plan Project of Guangdong Province (grant number 2016TQ03Z354).

554 **References**

- 555 [Ahmed, K., Shahid, S., Wang, X., Nawaz, N., and Khan, N.: Evaluation of gridded precipitation datasets over arid regions](#)
556 [of Pakistan. *Water*, 11, 210, 2019.](#)
- 557 [Bierhuizen, J.: Some observations on the relation between transpiration and soil moisture, *Netherlands Journal of*
558 \[Agricultural Science\]\(#\), 6, 94-98, 1958.](#)
- 559 Budyko, M. I.: *Climate and life*, Academic press 1974.
- 560 Caracciolo, D., Pumo, D., and Viola, F.: Budyko's based method for annual runoff characterization across different climatic
561 areas: an application to United States, *Water Resources Management*, 32, 3189-3202, 2018.
- 562 Cavanaugh, M. L., Kurc, S. A., and Scott, R. L.: Evapotranspiration partitioning in semiarid shrubland ecosystems: a two-
563 site evaluation of soil moisture control on transpiration, *Ecohydrology*, 4, 671-681, 2011.
- 564 Chen, X. and Sivapalan, M.: Hydrological basis of the Budyko curve: Data-guided exploration of the mediating role of soil
565 moisture, *Water Resources Research*, 56, e2020WR028221, 2020.
- 566 [Choudhury, B.: Evaluation of an empirical equation for annual evaporation using field observations and results from a](#)
567 [biophysical model. *Journal of Hydrology*, 216, 99-110, 1999.](#)
- 568 [Degefu, M. A., Bewket, W., and Amha, Y.: Evaluating performance of 20 global and quasi-global precipitation products](#)
569 [in representing drought events in Ethiopia I: Visual and correlation analysis. *Weather and Climate Extremes*, 35,](#)
570 [100416, 2022.](#)
- 571 [Du, X., Silwal, G., and Faramarzi, M.: Investigating the impacts of glacier melt on stream temperature in a cold-region](#)
572 [watershed: Coupling a glacier melt model with a hydrological model. *Journal of Hydrology*, 605, 127303, 2022.](#)
- 573 Ducharme, A., Laval, K., and Polcher, J.: Sensitivity of the hydrological cycle to the parametrization of soil hydrology in a
574 GCM, *Climate dynamics*, 14, 307-327, 1998.
- 575 Feng, X.: Global maps of seasonality indices, HydroShare [dataset], 2019.
- 576 [Fiedler, K. and Döll, P.: Global modelling of continental water storage changes—sensitivity to different climate data sets,](#)
577 [Advances in Geosciences](#), 11, 63-68, 2007.
- 578 [Frölicher, T. L., Fischer, E. M., and Gruber, N.: Marine heatwaves under global warming, *Nature*, 560, 360-364, 2018.](#)
- 579 Fu, B.: On the calculation of the evaporation from land surface, *Chinese Journal of Atmospheric Sciences*, 5, 23-31, 1981.
- 580 Gan, G., Liu, Y., and Sun, G.: Understanding interactions among climate, water, and vegetation with the Budyko
581 framework, *Earth-Science Reviews*, 212, 103451, 2021.
- 582 ~~Gao, M., Chen, X., Liu, J., and Zhang, Z.: Regionalization of annual runoff characteristics and its indication of co-~~
583 ~~dependence among hydro-climate-landscape factors in Jinghe River Basin, China, *Stochastic Environmental*~~
584 ~~*Research and Risk Assessment*, 32, 1613-1630, 2018.~~
- 585 Ghiggi, G., Humphrey, V., Seneviratne, S. I., and Gudmundsson, L.: GRUN: an observation-based global gridded runoff
586 dataset from 1902 to 2014, *Earth System Science Data*, 11, 1655-1674, 2019.
- 587 Goswami, U. P. and Goyal, M. K.: Relative Contribution of Climate Variables on Long-Term Runoff Using Budyko
588 Framework, in: *Water Resources Management and Sustainability*, Springer, 147-159, 2022.
- 589 GRDC: Watershed Boundaries of GRDC Stations / Global Runoff Data Centre, Federal Institute of Hydrology (BfG)
590 [dataset], 2011.
- 591 [Greve, P., Gudmundsson, L., Orłowsky, B., and Seneviratne, S. I.: Introducing a probabilistic Budyko framework,](#)
592 [Geophysical Research Letters](#), 42, 2261-2269, 2015.
- 593 Guan, X., Zhang, J., Yang, Q., and Wang, G.: Quantifying the effects of climate and watershed structure changes on runoff
594 variations in the Tao River basin by using three different methods under the Budyko framework, *Theoretical and*
595 *Applied Climatology*, 1-14, 2022.

596 Guo, A., Chang, J., Wang, Y., Huang, Q., Guo, Z., and Li, Y.: Uncertainty analysis of water availability assessment through
597 the Budyko framework, *Journal of Hydrology*, 576, 396-407, 2019.

598 Havranek, W. M. and Benecke, U.: The influence of soil moisture on water potential, transpiration and photosynthesis of
599 conifer seedlings, *Plant and Soil*, 49, 91-103, 1978.

600 [Hu, Z., Zhou, Q., Chen, X., Li, J., Li, Q., Chen, D., Liu, W., and Yin, G.: Evaluation of three global gridded precipitation
601 data sets in central Asia based on rain gauge observations, *International Journal of Climatology*, 38, 3475-3493, 2018.](#)

602 Jiao, L., Lu, N., Fang, W., Li, Z., Wang, J., and Jin, Z.: Determining the independent impact of soil water on forest
603 transpiration: a case study of a black locust plantation in the Loess Plateau, China, *Journal of Hydrology*, 572, 671-
604 681, 2019.

605 Kanishka, G. and Eldho, T.: Watershed classification using isomap technique and hydrometeorological attributes, *Journal
606 of Hydrologic Engineering*, 22, 04017040, 2017.

607 Kanishka, G. and Eldho, T.: Streamflow estimation in ungauged basins using watershed classification and regionalization
608 techniques, *Journal of Earth System Science*, 129, 1-18, 2020.

609 Kim, D. and Chun, J. A.: Revisiting a Two-Parameter Budyko Equation With the Complementary Evaporation Principle
610 for Proper Consideration of Surface Energy Balance, *Water Resources Research*, 57, e2021WR030838, 2021.

611 Lei, H., Yang, D., and Huang, M.: Impacts of climate change and vegetation dynamics on runoff in the mountainous region
612 of the Haihe River basin in the past five decades, *Journal of Hydrology*, 511, 786-799, 2014.

613 Li, D., Pan, M., Cong, Z., Zhang, L., and Wood, E.: Vegetation control on water and energy balance within the Budyko
614 framework, *Water Resources Research*, 49, 969-976, 2013.

615 ~~Li, H. Y. and Sivapalan, M.: Functional approach to exploring climatic and landscape controls on runoff generation: 2
616 Timing of runoff storm response, *Water Resources Research*, 50, 9323-9342, 2014~~

617 [Li, Y., Li, F., Shangguan, D., and Ding, Y.: A new global gridded glacier dataset based on the Randolph Glacier Inventory
618 version 6.0, *Journal of Glaciology*, 67, 773-776, 2021.](#)

619 Liang, S., Cheng, J., Jia, K., Jiang, B., Liu, Q., Xiao, Z., Yao, Y., Yuan, W., Zhang, X., and Zhao, X.: The global land
620 surface satellite (GLASS) product suite, *Bulletin of the American Meteorological Society*, 102, E323-E337, 2021.

621 Liu, J., You, Y., Zhang, Q., and Gu, X.: Attribution of streamflow changes across the globe based on the Budyko framework,
622 *Science of The Total Environment*, 794, 148662, 2021.

623 [Liu, J., Long, A., Deng, X., Yin, Z., Deng, M., An, Q., Gu, X., Li, S., and Liu, G.: The Impact of Climate Change on
624 Hydrological Processes of the Glacierized Watershed and Projections, *Remote Sensing*, 14, 1314, 2022a.](#)

625 Liu, Q. and Liang, L.: Impacts of climate change on the water balance of a large nonhumid natural basin in China,
626 *Theoretical and Applied Climatology*, 121, 489-497, 2015.

627 Liu, S., Wang, X., Zhang, L., Kong, W., Gao, H., and Xiao, C.: Effect of glaciers on the annual catchment water balance
628 within Budyko framework, *Advances in Climate Change Research*, 13, 51-62, ~~2022~~2022b.

629 [Metselaar, K. and de Jong van Lier, Q.: The shape of the transpiration reduction function under plant water stress, *Vadose
630 Zone Journal*, 6, 124-139, 2007.](#)

631 [Mezentsev, V.: Back to the computation of total evaporation, *Meteorologia i Gidrologia*, 5, 24-26, 1955.](#)

632 Milly, P. and Shmakin, A.: Global modeling of land water and energy balances. Part II: Land-characteristic contributions
633 to spatial variability, *Journal of Hydrometeorology*, 3, 301-310, 2002.

634 Nash, J. E. and Sutcliffe, J. V.: River flow forecasting through conceptual models part I—A discussion of principles,
635 *Journal of hydrology*, 10, 282-290, 1970.

636 Ning, T., Li, Z., and Liu, W.: Vegetation dynamics and climate seasonality jointly control the interannual catchment water
637 balance in the Loess Plateau under the Budyko framework, *Hydrology and Earth System Sciences*, 21, 1515-1526,
638 2017.

639 [NOAANCEI: Monthly National Climate Report for July 2011, NOAA National Centers for Environmental Information,](#)
640 [2011.](#)

641 [Padrón, R. S., Gudmundsson, L., Greve, P., and Seneviratne, S. I.: Large-scale controls of the surface water balance over](#)
642 [land: Insights from a systematic review and meta-analysis, *Water Resources Research*, 53, 9659-9678, 2017.](#)

643 Pedregosa, F., Varoquaux, G., Gramfort, A., Michel, V., Thirion, B., Grisel, O., Blondel, M., Prettenhofer, P., Weiss, R.,
644 and Dubourg, V.: Scikit-learn: Machine learning in Python, the *Journal of machine Learning research*, 12, 2825-2830,
645 2011.

646 Rau, P., Bourrel, L., Labat, D., Frappart, F., Ruelland, D., Lavado, W., Dewitte, B., and Felipe, O.: Hydroclimatic change
647 disparity of Peruvian Pacific drainage catchments, *Theoretical and applied climatology*, 134, 139-153, 2018.

648 [Reaver, N. G., Kaplan, D. A., Klammler, H., and Jawitz, J. W.: Theoretical and empirical evidence against the Budyko](#)
649 [catchment trajectory conjecture, *Hydrology and Earth System Sciences*, 26, 1507-1525, 2022.](#)

650 Rodell, M., Houser, P., Jambor, U., Gottschalck, J., Mitchell, K., Meng, C.-J., Arsenault, K., Cosgrove, B., Radakovich, J.,
651 and Bosilovich, M.: The global land data assimilation system, *Bulletin of the American Meteorological society*, 85,
652 381-394, 2004.

653 Roderick, M. L. and Farquhar, G. D.: A simple framework for relating variations in runoff to variations in climatic
654 conditions and catchment properties, *Water Resources Research*, 47, 2011.

655 [Salaudeen, A., Ismail, A., Adeogun, B. K., Ajibike, M. A., and Zubairu, I.: Evaluation of ground-based, daily, gridded](#)
656 [precipitation products for Upper Benue River basin, Nigeria, *Engineering and Applied Science Research*, 48, 397-](#)
657 [405, 2021.](#)

658 Schwarzel, K., Zhang, L., Montanarella, L., Wang, Y., and Sun, G.: How afforestation affects the water cycle in drylands:
659 A process-based comparative analysis, *Global Change Biology*, 26, 944-959, 2020.

660 ~~Singh, R., Archfield, S., and Wagener, T.: Identifying dominant controls on hydrologic parameter transfer from gauged to~~
661 ~~ungauged catchments—A comparative hydrology approach, *Journal of Hydrology*, 517, 985-996, 2014.~~

662 Sinha, J., Jha, S., and Goyal, M. K.: Influences of watershed characteristics on long-term annual and intra-annual water
663 balances over India, *Journal of Hydrology*, 577, 123970, 2019.

664 Sivapalan, M.: Process complexity at hillslope scale, process simplicity at watershed scale: Is there a connection?, EGS-
665 AGU-EUG Joint Assembly, 7973,

666 ~~Trancoso, R., Phinn, S., McVicar, T. R., Larsen, J. R., and McAlpine, C. A.: Regional variation in streamflow drivers~~
667 ~~across a continental climatic gradient, *Ecohydrology*, 10, e1816, 2017.~~

668 [Tixeront, J.: Prediction of streamflow, IAHS publication, 118-126, 1964.](#)

669 [Turc, L.: The water balance of soils. Relation between precipitation, evaporation and flow, *Ann. Agron.*, 5, 491-569, 1954.](#)

670 [UNEP: World atlas of desertification, United Nations Environment Programme \[dataset\], 1997.](#)

671 [Verhoef, A. and Egea, G.: Modeling plant transpiration under limited soil water: Comparison of different plant and soil](#)
672 [hydraulic parameterizations and preliminary implications for their use in land surface models, *Agricultural and Forest*](#)
673 [Meteorology, 191, 22-32, 2014.](#)

674 Vora, A. and Singh, R.: Satellite based Budyko framework reveals the human imprint on long-term surface water
675 partitioning across India, *Journal of Hydrology*, 602, 126770, 2021.

676 Walsh, R. and Lawler, D.: Rainfall seasonality: description, spatial patterns and change through time, *Weather*, 36, 201-
677 208, 1981.

678 Wang, D. and Tang, Y.: A one-parameter Budyko model for water balance captures emergent behavior in Darwinian
679 hydrologic models, *Geophysical Research Letters*, 41, 4569-4577, 2014.

680 Wang, F., Xia, J., Zou, L., Zhan, C., and Liang, W.: Estimation of time-varying parameter in Budyko framework using
681 long short-term memory network over the Loess Plateau, China, *Journal of Hydrology*, 607, 127571, 2022.

682 [Wang, H., Lv, X., and Zhang, M.: Sensitivity and attribution analysis of vegetation changes on evapotranspiration with the
683 Budyko framework in the Baiyangdian catchment, China, *Ecological Indicators*, 120, 106963, 2021.](#)

684 Wang, Y., Bredemeier, M., Bonell, M., Yu, P., Feger, K.-H., Xiong, W., and Xu, L.: Comparison between a statistical
685 approach and paired catchment study in estimating water yield response to afforestation, *Revisiting Experimental
686 Catchment Studies in Forest Hydrology:(Proceedings of a Workshop held during the XXV IUGG General Assembly
687 in Melbourne, June–July 2011, 3-11,*

688 Xu, X., Liu, W., Scanlon, B. R., Zhang, L., and Pan, M.: Local and global factors controlling water-energy balances within
689 the Budyko framework, *Geophysical Research Letters*, 40, 6123-6129, 2013.

690 Yang, D., Shao, W., Yeh, P. J. F., Yang, H., Kanae, S., and Oki, T.: Impact of vegetation coverage on regional water
691 balance in the nonhumid regions of China, *Water Resources Research*, 45, 2009.

692 Yang, H., Yang, D., Lei, Z., and Sun, F.: New analytical derivation of the mean annual water-energy balance equation,
693 *Water resources research*, 44, 2008.

694 [Yang, H., Qi, J., Xu, X., Yang, D., and Lv, H.: The regional variation in climate elasticity and climate contribution to runoff
695 across China, *Journal of hydrology*, 517, 607-616, 2014.](#)

696 Yao, J., Mao, W., Yang, Q., Xu, X., and Liu, Z.: Annual actual evapotranspiration in inland river catchments of China
697 based on the Budyko framework, *Stochastic Environmental Research and Risk Assessment*, 31, 1409-1421, 2017.

698 Yao, W., Xiao, P., Shen, Z., Wang, J., and Jiao, P.: Analysis of the contribution of multiple factors to the recent decrease
699 in discharge and sediment yield in the Yellow River Basin, China, *Journal of Geographical Sciences*, 26, 1289-1304,
700 2016.

701 Yu, K.-x., Zhang, X., Xu, B., Li, P., Zhang, X., Li, Z., and Zhao, Y.: Evaluating the impact of ecological construction
702 measures on water balance in the Loess Plateau region of China within the Budyko framework, *Journal of Hydrology*,
703 601, 126596, 2021.

704 Zhang, L., Dawes, W., and Walker, G.: Response of mean annual evapotranspiration to vegetation changes at catchment
705 scale, *Water resources research*, 37, 701-708, 2001.

706 [Zhang, L., Hickel, K., Dawes, W., Chiew, F. H., Western, A., and Briggs, P.: A rational function approach for estimating
707 mean annual evapotranspiration, *Water resources research*, 40, 2004.](#)

708 Zhang, S., Yang, Y., McVicar, T. R., and Yang, D.: An analytical solution for the impact of vegetation changes on
709 hydrological partitioning within the Budyko framework, *Water Resources Research*, 54, 519-537, 2018.

710 Zhou, G., Wei, X., Chen, X., Zhou, P., Liu, X., Xiao, Y., Sun, G., Scott, D. F., Zhou, S., and Han, L.: Global pattern for
711 the effect of climate and land cover on water yield, *Nature communications*, 6, 1-9, ~~2015~~2015a.

712 [Zhou, S., Yu, B., Huang, Y., and Wang, G.: The complementary relationship and generation of the Budyko functions,
713 *Geophysical Research Letters*, 42, 1781-1790, 2015b.](#)

714